

THESIS FOR THE DEGREE OF DOCTOR OF PHILOSOPHY

Effects of Steel Fibres on
Cracking in Reinforced Concrete

ANETTE JANSSON

Department of Civil and Environmental Engineering
Division of Structural Engineering
Concrete Structures
CHALMERS UNIVERSITY OF TECHNOLOGY
Gothenburg, Sweden, 2011

Effects of Steel Fibres on Cracking in Reinforced Concrete

ANETTE JANSSON

ISBN 978-91-7385-552-5

© ANETTE JANSSON, 2011

Doktorsavhandlingar vid Chalmers tekniska högskola

Ny serie Nr 3233

ISSN no. 0346-718X

Department of Civil and Environmental Engineering

Division of Structural Engineering

Concrete Structures

Chalmers University of Technology

SE-412 96 Gothenburg

Sweden

Telephone: + 46 (0)31-772 1000

Cover:

The cover picture shows the principle strategy for the study of tension and bond, see Sections 6.

Chalmers Repro Service

Gothenburg, Sweden, 2011

Effects of Steel Fibres on Cracking in Reinforced Concrete
ANETTE JANSSON

Department of Civil and Environmental Engineering
Division of Structural Engineering, Concrete Structures
Chalmers University of Technology

ABSTRACT

Although it is well known that fibre reinforcement acts as a crack arresting agent, there is still a need for deeper knowledge of the actual cracking behaviour, especially regarding cracks with widths smaller than 0.3mm. Today major fibre applications are as a replacement for the welded mesh in industrial floors, and as reinforcement in sprayed concrete. However, other applications exist and are investigated.

By combining experiments with finite-element analyses, the effects of fibres on cracking in conventionally reinforced, self-compacting, steel-fibre-reinforced concrete (SCSFRC) were studied. When studying the beginning of the cracking process, the tensile softening behaviour (σ - w relationship), and the bond stress-slip behaviour, which are the ones mainly affecting the cracking, are clearly of interest. Contradictory information on the effect of fibres on bond behaviour was found in the literature. Pull-out tests with short embedment length were thus carried out. The σ - w relationship may be obtained indirectly by inverse analysis, e.g. from wedge-splitting tests, or directly, from uniaxial tension tests (UTT); both approaches were used in this work. To investigate the cracking process, tension tests of tie elements were carried out, where, in addition to the load-deformation curves, a full-field strain measuring technique using Digital Image Correlation (DIC) was used to monitor the surface cracking.

It was found from the pull-out tests that, for the type and amount of fibres used here, the bond properties at the interface layer were neither reduced nor improved. There were indications, however, that the initial stiffness of the bond stress-slip curves was increased by the self-compacting concrete. The UTT and the tie element testing showed that the scatter was quite high regarding the number of fibres in a cut cross section. It was seen that fibre reinforcement markedly improves tension stiffening and, at a given load, the characteristic crack width is greatly reduced compared with plain concrete. The DIC gave good insight into the surface crack initiation and enabled the tension stiffening to be quantified by relating it to the characteristic crack widths. In addition, it was seen that the cracking load and first-peak tensile stress increased with an increasing amount of fibres.

The Finite element analyses of the beams and the tie elements revealed that the methodology used was versatile. It was found that the smeared crack model did not yield crack localization for materials with high fibre content ($V_f > 0.5\%$) if homogenous material properties were assumed. Instead a semi-meso approach was used; properties for plain concrete were assigned to randomly designated parts of the elements, while the remaining elements were assigned modified tensile properties. The modified properties were increased so that the average σ - w curve of one cross section corresponded to the average curve from the UTT. With the new approach, the load-elongation response agreed better with the experiments; crack localization was obtained and crack widths could be reasonably reproduced.

Keywords: Self-compacting, fibre-reinforced, bond, pull-out test, uniaxial tension test, tension stiffening, characteristic crack width, Digital Image Correlation

Stålfibrers effekt av på sprickprocessen i armerad betong

ANETTE JANSSON

Institutionen för bygg- och miljöteknik

Konstruktionsteknik, Betongbyggnad

Chalmers tekniska högskola

SAMMANFATTNING

Det är väl känt att fibrer reducerar sprickor, trots det finns fortfarande ett behov av ökad kunskap angående sprickprocessen, särskilt för sprickvidder mindre än 0,3mm. Idag används fiberarmering i huvudsak som ersättning för armeringsnät i industrigolv och som armering i sprutbetong. Andra användningsområden finns och undersöks.

Genom att kombinera laboratorieförsök och finit elementanalys, har fibrers effekt på sprickor i armerad, självkompakterande, stålfiberarmerad betong, studerats. Korrekta materialparametrar är viktiga då första skedet av sprickprocessen ska undersökas; särskilt viktiga är mjuknadedelen i dragspänning-sprick ($\sigma-w$)-förhållandet och vidhäftnings-glidningsförhållandet, eftersom det i huvudsak är dessa som påverkar sprickprocessen. En litteraturstudie påvisade motsägande information angående fibrers effekt på vidhäftningsmekanismerna, därför utfördes utdragsförsök med kort ingjutningslängd. $\sigma-w$ -förhållandet kan erhållas indirekt t.ex. från kilspräckförsök, eller direkt genom enaxiellt dragförsök; båda metoderna användes i projektet. För att undersöka sprickbildningsprocessen utfördes enaxiella dragförsök på armerade betongprismor (dragstag). Utöver uppmätt last-deformationskurva, gjordes en global mätning av yttöjningarna med Digital Image Correlation (DIC) teknik.

Resultat från utdragsförsöken visade att använd fibertyp och fibermängd varken förbättrade eller försämrade vidhäftningsegenskaperna i gränsskiktet betong-stål; däremot erhöles en effekt motsvarande den från konventionell tvärarmering efter spjälksprickor uppstått. Det fanns indikationer på att den självkompakterande betongen gav ökad initiell styvhet i vidhäftning-glidningskurvan. Dragförsöken påvisade en hög spridning av antalet fibrer i ett tvärsnitt. Fiberarmering visade sig tydligt öka betongens bidrag i dragna delar, och vid given belastning sågs en markant minskning av karakteristisk sprickvidd jämfört med betong utan fibrer. DIC-tekniken gav, god insikt i sprickinitieringen på ytan av dragstagen, och även möjlighet att kvantifiera betongens bidrag genom att relatera den till karakteristisk sprickvidd. Dessutom sågs en ökad spricklast och en ökning av draghållfastheten vid ökande fiberinnehåll.

FEA av dragstagen och balkarna visade den använda metodikens mångsidighet. Den använda sprickmodellen visade sig olämplig för material med högre fiberinnehåll ($V_f > 0.5\%$), om homogena materialegenskaper antagits. Istället användes en metod där materialegenskaper för betong utan fibrer gavs till slumpartat valda betongelement i modellen; resterande element fick modifierade dragegenskaper. De modifierade egenskaperna innebar ökad kapacitet så att tvärsnittets $\sigma-w$ medelkurva motsvarade försöksresultaten från de enaxiella dragförsöken. Med denna metod erhöles bättre överrensstämmelse mellan analys och försök gällande last-deformation, och spricklokalisering erhöles.

Nyckelord: Självkompakterande, fiberarmerad, vidhäftning, utdragsförsök, enaxiellt dragförsök, tension stiffening, karakteristisk sprickvidd, Digital Image Correlation

Contents

ABSTRACT	ERROR! BOOKMARK NOT DEFINED.
SAMMANFATTNING	II
CONTENTS	III
PREFACE	V
NOTATIONS	X
1 INTRODUCTION	1
1.1 Background	1
1.2 Aim, Scope and Limitations	3
1.3 Original Features	3
1.4 Outline of the Thesis	4
2 DESIGN, ANALYTICAL METHODS, AND FIBRE DISTRIBUTION	5
2.1 Design methods for Fibre-Reinforced Concrete	5
2.2 Analytical methods for fibre-reinforced concrete	6
2.3 The effect of fibre distribution	7
3 EXPERIMENTAL PROGRAMMES	10
4 NON-LINEAR FINITE ELEMENT MODELLING	13
4.1 Tensile behaviour	13
4.1.1 The tensile strength	13
4.1.2 The softening curve	13
4.1.3 Stress-strain (σ - ε) relationship	14
4.2 Compression curve and Young's modulus	15
4.3 Bond behaviour	15
5 STUDY OF SPLITTING AND BENDING	17
5.1 Material properties	17
5.2 Wedge-splitting tests: Experiments	17
5.3 Wedge-splitting tests: Non-linear analysis	19
5.4 4-point beam bending: Experiments	22
5.5 4-point beam bending: Non-linear analysis	23
6 STUDY OF TENSION AND BOND	26
6.1 Material properties	26
6.2 Uniaxial Tension Tests	27
CHALMERS , <i>Civil and Environmental Engineering</i>	III

6.3	UTT analysis	28
6.4	Pull-out test with short embedment length: Experiments	29
7	REFERENCES	46

Preface

This thesis is done within a research project concerning cracking of conventionally reinforced, self-compacting steel-fibre-reinforced concrete, and was carried out at the Department of Structural Engineering, Concrete Structures, Chalmers University of Technology, Sweden from February 2006 to May 2011. A donation from Thomas Concrete Group AB (TCG), Göteborg, financed the project.

The project was carried out with Professor Kent Gylltoft as examiner and main supervisor, whom I thank for all your good advice regarding technical matters and especially for providing a stimulating environment for your staff. My supervisors, Ingemar Löfgren and Karin Lundgren, are greatly appreciated for their help with planning the tests and their extensive knowledge came in handy when writing my papers. I would like to show Karin extra gratitude for all help with the analyses in Diana and for her ability to devise good structures. Many thanks go to Mathias Flansbjer at SP for his invaluable knowledge and contributions to both the tie element and the uniaxial tension testing, as well as for being a co-author of Paper III. I would also like to thank my colleagues for their co-operation and involvement, with special thanks to my “next-door neighbour”, Kamyab Zandi Hanjari, for his never ending enthusiasm in helping me with the mysteries of Diana. I am grateful to Yvonne and Lisbeth, who have been most helpful in all that regards institutional matters.

Professor Tomas Kutti from TCG has been most helpful, giving good advice during meetings and when reading my papers, and I want to thank Ola Johansson (TCG) and Professor Jan Bröchner for helpful advice at our meetings. Special thanks go to the members of my reference group: P.O Svahn from Skanska Teknik, Göteborg, and Jonas Magnusson from NCC Teknik, Göteborg; without their invaluable advice this thesis would have been very thin.

To my family I can only say, thanks for your patience!

Finally, it should be noted that the tests could never have been conducted without the sense of high quality and professionalism of the laboratory staff at both SP and Chalmers.

Göteborg May 2011

Anette Jansson

LIST OF PUBLICATIONS

This thesis is based on the work contained in the following papers, referred to by Roman numerals in the text.

- I. Jansson A., Löfgren I., Gylltoft K. (2008). Design Methods for Fibre-Reinforced Concrete: a State-of-the-art Review, *Nordic Concrete Research*, Publication No. 38. pp. 31-46.
- II. Jansson A., Löfgren I., Gylltoft K. (2010). Flexural Behaviour of Members with a Combination of Steel Fibres and Conventional Reinforcement, *Nordic Concrete Research*, NCR 2010 publication No. 42, pp.155-171.
- III. Jansson A., Flansbjer M., Löfgren I., Lundgren K., Gylltoft K. (2011). Experimental Investigation of Surface Crack Initiation, Propagation and Tension Stiffening in Self-Compacting Steel-Fibre Reinforced Concrete, submitted to *Materials and Structures*.
- IV. Jansson A., Löfgren I., Lundgren K., Gylltoft K. (2011). Bond of Reinforcement in Self-Compacting Steel-Fibre Reinforced Concrete, submitted to *Magazine of Concrete Research*.
- V. Jansson A., Löfgren I., Lundgren K., Gylltoft K. (2011). Cracking in Self-Compacting Steel-Fibre Reinforced Concrete: Finite Element analysis, to be submitted to *Concrete Structures*.

AUTHOR'S CONTRIBUTIONS TO JOINTLY PUBLISHED PAPERS

The contribution of the author of this doctoral thesis to the appended papers is described here.

- I. Responsible for the writing and for the major part of the planning of the paper.
- II. Responsible for the writing and for a major part of the planning of the paper. Carried out the FE analyses.
- III. Responsible for the main part of the writing and planning of the paper. Planned a major part of and participated in the experiments.
- IV. Responsible for the writing and for the main part of the planning of the paper. Planned and were responsible for the execution of the experiments. Carried out the FE analyses.
- V. Responsible for the writing, and for the main part of the planning of the paper. Carried out the FE analyses.

OTHER PUBLICATIONS RELATED TO THE THESIS

Licentiate Thesis

Jansson, A. (2008). Fibres in reinforced concrete structures, analysis, experiments and design. Civil and Environmental Engineering. Göteborg, 2008, Chalmers University of Technology. Licentiate Thesis: pp.70.

Conference Papers

Jansson A., Löfgren I., Gylltoft K. (2007). A Fracture Mechanics Approach to Material Testing and Structural Analysis of FRC Beams. *The Proceedings of the 6th International Conference on Fracture Mechanics of Concrete and Concrete Structures*, Catania, Italy, 17-22 June 2007. pp. 1491-1496.

Jansson A., Löfgren I., Lundgren K., Gylltoft K. (2008). Material Testing and Structural Analysis of FRC Beams – A Fracture Mechanics Approach. *7th RILEM International Symposium on Fibre Reinforced Concrete Design and Applications*. Chennai, India. September 2008.

Reports

Jansson A. (2007). Analysis and Design Methods for Fibre Reinforced Concrete: A State-of-the Art Report. Chalmers Report No. 2007:16

Notations

Roman upper case letters

E	Modulus of elasticity of matrix
F_{sp}	Splitting load in the wedge-splitting test
F_v	Vertical load in the wedge-splitting test
G_F	Specific fracture energy
G_f	Specific energy dissipated during fracture
l_f	Fibre length
M	Bending moment
N	Normal force
N_b	Number of bridging fibres
$N_{f,WST}$	Number of fibres per unit area in a fractured specimen
V_f	Volume fraction of fibres

Roman lower case letters

a_1	Initial slope of the bi-linear σ - w relationship
a_2	Second slope of the bi-linear σ - w relationship
b_2	Intersection of the bi-linear σ - w relationship and the y-axis
d_f	Diameter of fibre
f_a	Adhesion
$f_{c(m)}$	Compressive strength (mean value)
f_{sp}	Splitting tensile strength
$f_{t(m)}$	Tensile strength (mean value)
f_y	Yield stress of reinforcing steel
f_u	Ultimate tensile capacity of reinforcing steel
h	Height of beam section, or crack-band width
l_{ch}	Characteristic length
l_f	Length of fibre
s	Length of non-linear hinge region
s_{rm}	Average crack spacing
w	Crack opening

Greek letters

α	Wedge angle in the wedge-splitting test, or fibre orientation factor
β	Factor for time dependency; or coefficient representing average stress in the concrete between cracks (bond factor)
δ	Deflection or displacement
ε	Strain
κ	Hardening parameter in bond model
ν	Poisson's ratio
ρ	Reinforcement ratio
μ	Coefficient of friction
θ	Crack opening angle
η	Dilatation parameter in bond model

η_b	Fibre efficiency factor
σ	Stress
$\sigma(w)$	Stress as a function of crack opening
τ_b	Bond strength

Acronyms

AR-GFRC	Alkali Resistant Glass Fibre Reinforced Concrete
<i>CMOD</i>	Crack Mouth Opening Displacement
CoV / COV	Coefficient of Variance
EC2	Eurocode 2
ECC	Engineered Cementitious Composite
FEA	Finite Element Analysis
FEM	Finite Element Method
FRC	Fibre-Reinforced Concrete
GFRC	Glass Fibre Reinforced Concrete
HSC	High-Strength Concrete
HPFRCC	High-Performance Fibre-Reinforced Cementitious Composite
PVA	Polyvinyl acetate
RC-65/35	Specification of Dramix [®] fibre (65/35 = aspect ratio / length)
SFRC	Steel Fibre-Reinforced Concrete
SCC	Self-Compacting Concrete
SCSFRC	Self-Compacting Steel-Fibre-Reinforced Concrete
SIFCON	Slurry Infiltrated Fibre Concrete
SIMCON	Slurry Infiltrated Mat Concrete
WST	Wedge-Splitting Test
UTT	Uniaxial Tension Test
4-PBT	4-point beam bending test

1 Introduction

1.1 Background

The advantages of using fibres as reinforcement have been known since ancient times; e.g. 3500 years ago, sun-baked bricks were reinforced with straw. In modern times, in the early 1900s, asbestos cement was the first widely used manufactured composite, Bentur and Mindess (2006). In the 1960s, research on fibre-reinforced concrete was already advancing fast, and at the present time, fibres of various kinds are used to reinforce concrete in structural applications. Due to its high stiffness, the steel fibre is probably the most commonly used fibre material. However, synthetic fibres are gaining ground, and new materials are under continuous development.

The fibre-reinforced concrete materials may be classified as strain hardening or strain softening, to a large extent depending on the amount of fibres added, see e.g. Naaman and Reinhardt (1996), RILEM TC 162-TDF (2002) and Naaman and Reinhardt (2006).

Strain hardening is recognized by an increasing tensile stress after the first cracking, and it is accompanied by multiple cracking; strain-softening materials exhibit a decreasing tensile stress after the first cracking, see Figure 1.1. Strain softening materials are composed of moderate amounts of fibre, typically $V_f < 1.0\%$ by volume. They have become quite popular in the construction of industrial floors and are frequently used for tunnel linings (as sprayed concrete), see e.g. Kooiman (2000). The benefits of a strain-softening, fibre-reinforced material, as opposed to plain concrete, is mainly the greater possibility to control the size of the crack widths; thus it may play a major role from the point of view of durability. That is, smaller crack widths will delay the initiation of corrosion of the conventional reinforcement and consequently increase the possibility of a longer life span of the structure.

In the past decade, self-compacting, fibre-reinforced concrete (SCFRC), has attracted increased scientific attention, see e.g. Groth (2004), Grünewald (2004), Löfgren (2005), Carlswärd (2006), Schumacher (2006), Dössland (2008) and da Cunha (2010). With the use of SCFRC, the concrete is able to fill the mould driven by its own weight, thus avoiding the settling of fibres and aggregates, which may be caused by vibration. SCC properties are achieved by optimizing the matrix in terms of: filling ability, passing ability and segregation resistance, e.g. Grünewald (2004).

Strain hardening may be obtained by increasing the amount of fibre, although this is not quite as straightforward as it may appear. For the slender fibres that are preferred for improved toughness, the reduced workability at increasing amounts of fibre, limits the maximum amount of fibres that can be incorporated in the FRC mix. Although this can be overcome by different techniques, e.g. by reducing the aggregate size, increasing the paste content (water, cement, mineral additions and fine particles) and introducing super-plasticizers, or by pre-placing the fibres, as in SIFCON (slurry infiltrated fibre concrete) and SIMCON (slurry infiltrated mat concrete), these techniques are quite costly.

By optimising the different components of the FRC, strain hardening may be achieved without simply an increase in fibre volume. Methods for obtaining strain-hardening composites with a normal strength matrix and moderate fibre content of about 2 % by volume, were developed by Li and co-workers at Michigan University. This type of composite was named Engineered Cementitious Composites (ECC), see Bentur and Mindess (2006), Li et al. (1995) and Fischer and Li (2006). To meet the criteria for

ECC, the bond strength between the fibre and matrix must be controlled. Furthermore, for a given fibre content, the distribution of the fibres is significant for maximising the ductility. An uneven distribution reduces the ultimate strain of the composite.

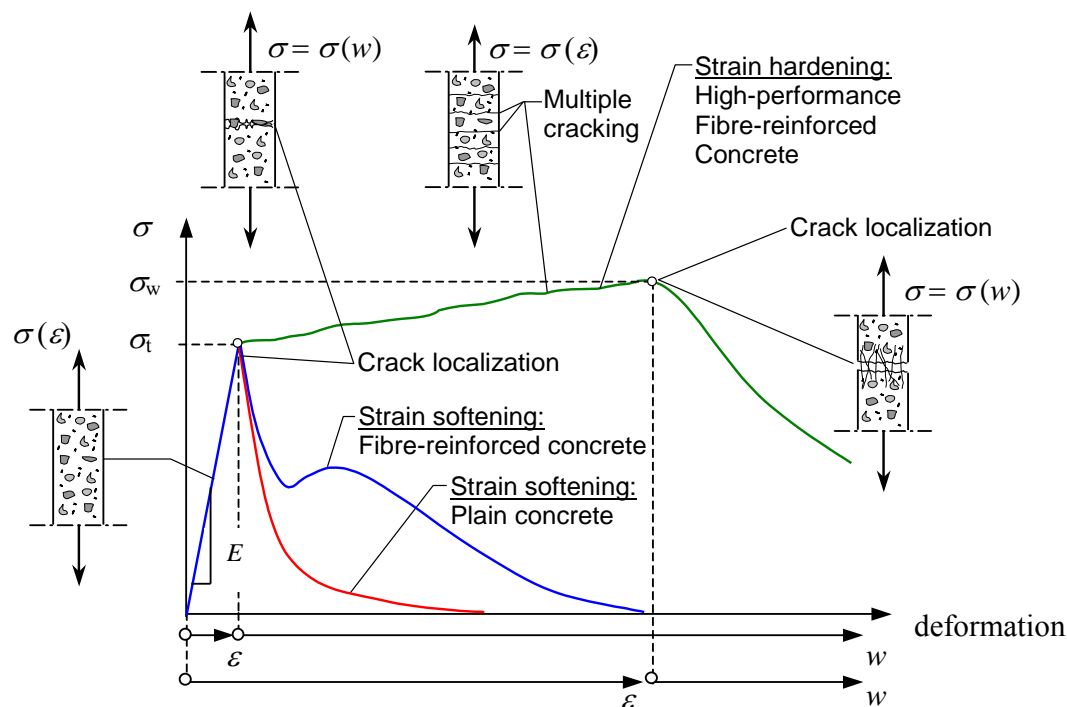


Figure 1.1 Difference in tensile behaviour for cement-based materials, from Löfgren (2005).

Rossi et al. (1987) distinguished between the different stages of crack formation (micro and macro). Based on this, the concept of hybrid reinforcement was proposed in terms of a large volume of short steel fibres to control micro-cracking and long fibres to bridge macro-cracks, Bentur and Mindess (2006). Bentur and Mindess refer to Banthia and Gupta (2004), who classified hybrid synergies into three groups. Each group includes one fibre type that provides toughness. This fibre is then combined with one of the following: fibres that provide strength; micro fibres that provide early crack control; or a type of fibre that changes the properties of the fresh mix. Banthia et al. (1993) studied restrained shrinkage cracking in FRC with fibre-volume fractions $V_f \approx 1\%$. They found that micro-fibres (length $< 20\text{mm}$) reduced the crack widths but were unable to induce multiple cracking. Macro-fibres (length $< 25\text{mm}$), on the other hand, distributed cracking effectively although without the capacity to delay the development of micro-cracks. Akkaya et al. (2000) tested extruded cement composites reinforced with 3% by volume of 2mm or 6mm-long fibres. They reported enhanced residual behaviour with multiple cracks from the composite with 2mm fibres, while the composite with 6mm fibres did not exhibit multiple cracking. This was explained by the better dispersion of the 2mm fibres.

From the point of view of durability it is essential to control the cracking process and, moreover, to be able to predict crack width and crack pattern and to design a structure that exhibits the desired behaviour. This behaviour depends of course on a number of different factors, such as: the type of structure and its size, type of concrete and amount and type of reinforcement and, not least, the casting procedure. In general, large amounts of conventional reinforcement are needed to achieve crack control, especially in structures where only very small crack widths ($w \leq 0.1 \text{ mm}$) are allowed.

Negative effects of large amounts of reinforcement are: structural dimensions must often be larger than what is needed for load bearing capacity in order to make space for all the steel; the heavy labour required in placing it; and the difficulties in pouring the concrete past the tightly placed reinforcement bars of the steel cage. These drawbacks may be reduced or even completely avoided by using fibres in combination with, or instead of, the conventional reinforcement.

1.2 Aim, Scope and Limitations

The aim of this work was to deepen knowledge of crack initiation and the initial crack growth at relatively low load levels in concrete members reinforced with a combination of steel fibres and conventional reinforcement. The thesis concerns cracking in the serviceability limit state; the effects of different amounts of one type of steel fibre have been studied. In a preliminary study, 4-point beam bending tests were carried out with a minimum of conventional reinforcement (rebars), diameter $\phi 6$ and $\phi 8$ mm. The beams were modelled in 2D using non-linear finite element analyses. The tensile softening (σ - w) curve was obtained through inverse analysis on results from wedge-splitting tests, which were performed in conjunction with the beam tests. Time-dependent effects such as creep and shrinkage were not considered.

The results of performed pull-out tests were used to calibrate a bond model proposed by Lundgren (2005); this model takes into account both tangential and normal deformation relative to the rebar and the corresponding tractions. Results from UTT and the calibrated bond model were used as input for 3D non-linear finite element analyses of the tie elements. Rebars of size $\phi 16$ mm were used for the pull-out and the tie element tests.

Self-compacting fibre-reinforced concrete was used in all tests, as this type of concrete has the benefits of improving the mechanical properties (e.g. bond and strength), allowing larger amounts of fibre to be added and reducing the amount of work required to compact the concrete. Moreover, this type of concrete also eliminates settling of the fibres due to vibration, although it may cause other types of orientation effects. With respect to bond properties, comparisons with conventional vibrated concrete were made by referring to earlier calibrations of the bond model used in the finite element analyses and comparing with the bond model suggested in CEB-FIP model Code 2010.

1.3 Original Features

While the Digital Image Correlation (DIC) technique has been available for many years, only a few reports were found in the literature on the use of DIC to monitor displacement fields in concrete. In the project, at the same time that the load-elongation curve was recorded in the tie element testing, the cracking was monitored by a full-field strain measuring technique using DIC. To the author's knowledge, there are no reports in the literature on this type of combination with FEM. Moreover, there are still relatively few studies being conducted and reported in which the uniaxial tension properties are determined and the fibre wall effect have been minimized. In addition, the study also comprises the bond-slip behaviour.

1.4 Outline of the Thesis

The thesis consists of 5 papers and an introductory part which gives a background to the subjects treated in the papers. *Chapter 1* gives a general background to fibre reinforcement; the aim, scope and limitations of the work, together with a description of the original features, are also presented. *Chapter 2* and paper I give a short introduction to the status of available methods for design and analysis of fibre-reinforced concrete (FRC). Areas which may affect the use of FRC are pointed out, e.g. fibre dispersion, and orientation of fibres. In addition, in Paper II, different proposals for calculation of average crack spacing are compared with experimental results and with results from finite element analyses.

In *Chapter 3*, the two experimental programmes, conducted within the project, are described; *Chapter 4* gives a presentation of each of the parameters needed for the finite element analyses that were performed in conjunction with the experiments.

Chapter 5 gives an overview of the experiments and FE analyses, performed within the first experimental study, regarding flexure and splitting; Paper II treats the effect of fibres on flexural behaviour. The FE analyses were based on estimated material parameters; the stress-crack opening relationship was obtained implicitly based on wedge-splitting tests and inverse analysis, and the bond stress-slip relationship was adopted from suggestions for plain concrete, found in the literature.

In *Chapter 6*, the second experimental study, together with FE analyses of the experiments, is described. This study regards tension and bond, and the material parameters used in the FEA, were obtained explicitly through: pull-out tests with short embedment length, and uniaxial tension tests (UTT) on notched cylinders. Tension tests on reinforced prisms were carried out, with the purpose of evaluating the cracking process with FEA based on the explicitly obtained material parameters. For these tests a digital image correlation (DIC) technique was used to monitor the surface strains during the testing. Paper III treats the experimental part of the UTT and the tension tests on reinforced concrete prisms. In Paper IV the pull-out tests are evaluated, and based on the results, a bond model for the FEA, developed by Lundgren (2005), is calibrated. The calibrated model, together with the UTT results, is used in FEA of the reinforced concrete prisms; this is treated in Paper V. A modified approach for cracking is proposed for materials with a residual tensile capacity close to hardening; this was used in the FE evaluation of the reinforced concrete prisms.

Chapter 7 discusses the difficulties with the choice of crack band width, which is needed when using a smeared approach for cracking in the FEA. The crack band width is the length over which the crack should be smeared out. This is also treated in Paper V. *Chapter 8* gives final conclusions and suggestions for further research.

2 Design, Analytical Methods, and Fibre Distribution

2.1 Design methods for Fibre-Reinforced Concrete

At the time this work on steel fibre effects began, test methods were available together with proposals for design methods for fibre-reinforced concrete (FRC), but nothing existed that was completely accepted and agreed upon within the concrete community. Paper I, based on the state-of-the-art report by Jansson (2007), briefly describes some of the design proposals available at the time, e.g. the Italian proposal by Ascione et al. (2006), the proposal made by the Swedish Concrete Society (1997) and the Norwegian proposal made by Thorenfeldt et al. (2006). The interest in fibres as reinforcement can be seen in the numerous workshops and conferences specifically focusing on this topic, e.g. Workshop proceeding no 2 (2001), Workshop proceeding no 4 (2003) and the FRC workshop (2007) at the FRAMCOS 6 Conference in Catania, Italy. At present, the first draft of the Model Code (2010) is on the bookshelves and, to some extent, this edition includes fibre-reinforced concrete. For the continued work within the project, it was realized that most of the current literature on FRC concerns the effect of fibres on the load-bearing capacity and increased ductility: Barr and Hasso (1985), Gopalaratnam et al. (1991), Banthia and Sheng (1996), who also made an attempt to quantify crack growth resistance, Pereira et al. (2004), Song and Hwang (2004) and Barros et al. (2005). Although several approaches to analytical descriptions can be found for analysing the flexural behaviour of FRC, see Section 2.2, there is still a gap in the literature: that of small crack widths.

The crack width depends among other factors on the crack spacing, and it was concluded by Vandewalle (2000) that the formulation for crack spacing found in EC2 (1991) was not applicable to FRC. In the modified proposals for the calculation of crack spacing in FRC by RILEM (2003) and in the Italian design draft for FRC by Ascione, Berardi et al. (2006), the aspect ratio (ratio of fibre length to fibre diameter) was taken into account. By multiplying the formula for crack spacing in plain concrete given in EC2 (1991) by the factor $(50 d_f / l_f)$, the contribution of the fibre to reduced crack spacing was assumed to have been accounted for. However, the actual fibre content was not. Hence, a fibre-volume fraction $V_f = 0.25\%$ would yield the same crack spacing as $V_f = 1.0\%$. Löfgren (2007) realized this and proposed a different approach in which the amount of fibre was accounted for by including the tensile residual capacity, f_{ft_res} , in the calculation of crack spacing. His approach was evaluated and compared with the RILEM approach, with results from 4-point beam-bending tests and with finite element analyses of beam tests, see Paper II. It was found that the approach of Löfgren yielded the best agreement with the experiments, followed by that of the FEA. The RILEM approach was unable to capture the decreasing crack spacing with increasing fibre content. Modifications have since been made and, according to Model Code 2010, the design crack width, w_d , in FRC with conventional reinforcement can be calculated as:

$$w_d = \frac{1}{2} \cdot \frac{\phi_s}{\rho_{s.ef}} \cdot \frac{(f_{ctm} - f_{Ftism})}{\tau_{bm}} \cdot \frac{1}{E_s} \cdot (\sigma_s - \beta \cdot \sigma_{sr} + \eta_r \cdot \varepsilon_r \cdot E_s) \quad (2.1)$$

where ϕ_s is the rebar diameter,

$$\rho_{s.ef} \text{ is the reinforcement ratio} = A_s / A_{c_ef},$$

in which A_s is the area of the reinforcement bar, and $A_{c_{ef}}$ is the effective area of the concrete cross section,

τ_{bm} is the mean bond strength between rebar and concrete,

E_s is the elastic modulus of the rebar,

σ_s is the steel stress in a crack,

β is an empirical coefficient to assess the mean strain over $l_{s,max}$,

$l_{s,max}$ is the length over which slip between concrete and steel occurs,

σ_{sr} is maximum steel stress in a crack in the crack formation stage,

η_r is a coefficient accounting for the shrinkage contribution,

ε_r is the strain at the onset of cracking and

f_{ctm} is the mean axial tensile strength of the concrete,

$$f_{Ftsm} = 0.45f_{R1},$$

where f_{R1} is the residual flexural tensile stress in the test specimen at crack mouth opening displacement, CMOD = 0.5mm, in a notched beam bending test. From the measured load, f_{R1} is calculated as:

$$f_{R1} = \frac{3 \cdot F_{0.5} \cdot l}{2 \cdot b \cdot h_{sp}^2} \quad (2.2)$$

in which $F_{0.5}$ is the load measured at CMOD = 0.5mm, b is the width of the specimen, h_{sp} is the height of the specimen minus the notch depth and l is the span length.

Compared with the earlier suggestions, it is seen that the new formula considers the residual stress, f_{Ftsm} (in which the fibre volume and fibre aspect ratio are implicitly included). The new formula is compared with the previous comparisons in Section 5.4.

2.2 Analytical methods for fibre-reinforced concrete

For plain concrete reinforced solely with conventional reinforcement, the tensile behaviour up to cracking is dictated mainly by the concrete; after cracking (for crack widths larger than $> 0.2 - 0.3$ mm), the tensile capacity of the reinforcement is utilised. Fibre-reinforced concrete on the other hand may exhibit considerable residual capacity in tension, and this increased ductility must be taken into account when the material is analysed.

As regards the flexural behaviour of FRC, several approaches have been proposed: for purely analytical models, see Ezeldin and Shiah (1995), who developed an analytical algorithm to evaluate the moment-curvature and load-deflection behaviour of SFRC beams reinforced with conventional rebars, and Lok and Pei (1998; Lok and Xiao (1999), who derived a theoretical expression to determine the cracking and the ultimate strength of SFRC.

With the introduction of fibre reinforcement, the combination of fracture mechanics and finite element modelling became a concept that attracted interest among researchers in the field. A semi-analytical model was developed by Zhang and Stang (1998); using non-linear FEM with the discrete crack approach, they investigated the

flexural behaviour of SFRC beams. Barros and Figueiras (2001) used non-linear finite element analyses to evaluate deflection and cracking in slabs on grade. They concluded that fibre reinforcement affects the post-peak behaviour in both tension and compression by making it more ductile. Based on experimental work with steel fibre-reinforced concrete (SFRC) and recommendations for plain concrete, e.g. fracture energy by RILEM and strain at peak stress by CEB-FIP Model Code 1990, they developed analytical formulations for the post-peak parts of the stress-strain relationships for tension and compression of SFRC. Furthermore, Kanstad and Dössland (2004) tested and modelled beams designed for moment failure; Sorelli et al. (2005) conducted uniaxial and bending tests on hybrid SFRC and simulated them; and Tlemat et al. (2006) performed inverse analyses to derive the tensile softening curve for SFRC; see also Elsaigh (2007), who used an analytical method to determine the tensile stress-strain response and used it in non-linear FEM of SFRC beams and ground slabs. Burger (2006) modelled SFRC tunnel segments and evaluated some of the crack models available in Diana and Abaqus; Plizzari and Tiberti (2007) modelled the structural behaviour of SFRC tunnel segments. Susetyo (2009) carried out experiments and FE modelling based on the VecTor2 non-linear FEM programme, and investigated the use of fibre reinforcement for shrinkage crack control of prestressed, precast segmental bridges. The VecTor2 program encompasses the variable Engagement Model 8VEM developed by Voo and Foster (2003).

As can be seen, the approach of combining non-linear fracture mechanics with FEM is now well established; it has proved to yield useful results in comparisons of numerical results with experimental results of fibre-reinforced concrete structures. Thus, for the work in this project, all of the laboratory tests were evaluated using a combination of fracture mechanics and non-linear finite element modelling.

2.3 The effect of fibre distribution

As expected, the fibre distribution has a major effect on the residual capacity, which is why it is important to be able to control this. Akkaya et al. (2001) found that the cracking stress was affected by the fibre-free areas in the cross sections since they act as defects in the material. Fibre distribution and orientation have been found to depend on many factors, including: casting and placement technique, specimen size, fibre size, geometry and fibre content, and maximum aggregate size, Robins et al. (2003), Grünewald (2004) and Dössland (2008).

Sorelli and Toutlemonde (2005) drilled cylinders from an SFRC tunnel segment, Figure 2.1, and tested them in uniaxial tension. They found that the specimens belonging to column C and row 1 exhibited a significantly higher average residual stress than the others; i.e. the fibre distribution within the specimen was noticeably uneven. An uneven fibre distribution was also found in the tests conducted in this work; counting fibres in cross sections (cut and cracked) revealed that the scatter in terms of coefficient of variation (COV) varied from 16% to 57%.

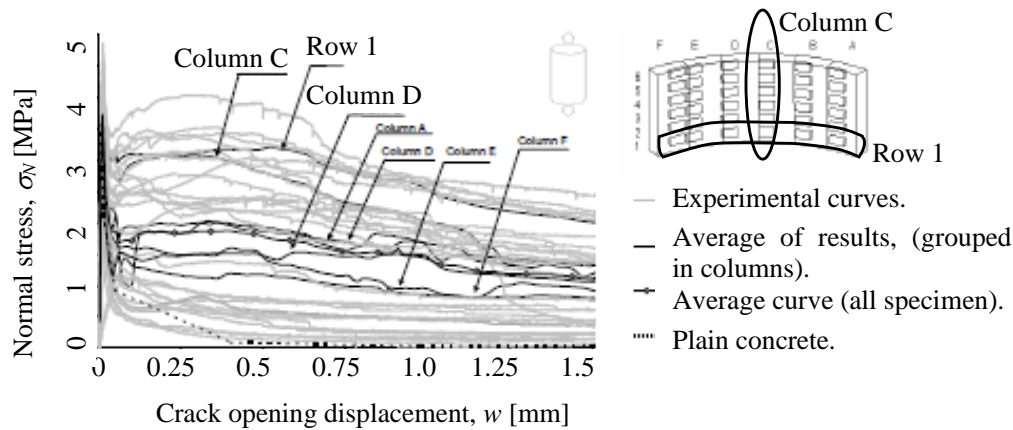


Figure 2.1 Experimental tensile test response in terms of stress-crack opening displacement (σ_N-w), modified from Sorelli and Toutlemonde (2005).

Small fibre-volume fractions exhibit a larger scatter in fibre distribution than higher fibre-volume fractions, e.g. Kooiman (2000) and Lambrechts (2004). In addition, owing to workability, there exists a critical upper limit of the amount of fibre that can be added directly to the concrete. The workability problem can be overcome by special techniques, such as SIFCON (slurry infiltrated fibre concrete) and SIMCON (slurry infiltrated mat concrete). For SIFCON, the steel fibres are placed in a mould, with fibre volumes of typically 4 to 12%, and the concrete paste is then infiltrated. While the SIFCON material is labour intensive in terms of placing the fibres, the SIMCON material uses the same type of fibres as that used in SIFCON but here they are placed as a pre-made mat, thus allowing for higher slenderness of the fibres, Bentur and Mindess (2006).

These techniques are quite costly and such large fibre-volume fractions are furthermore not relevant when the reinforcement is intended for crack control; thus, the problem of large scatter for small fibre-volume fractions remains.

Another issue related to the fibre distribution is the orientation of the fibres. A fibre that is oriented perpendicular to the loading direction does not contribute to the stress transfer across a crack. The casting method, the flow ability of the mix and the size of the mould have a great impact on the final alignment of the fibres. Robins, Austin et al. (2003) investigated fibre distribution in steel fibre-reinforced sprayed concrete and made comparisons with conventional cast fibre concrete. The test variables investigated were: fibre volume, beam depth and the method of placement (i.e. casting or spraying). The cast beams were produced by moulds, $100 \times 100 \times 500\text{mm}^3$, while the sprayed beams were cut from larger cast panels, $600 \times 600 \times 100\text{mm}^3$. All specimens were then cut to obtain a cross sectional height of the beams between 60 and 85 mm. Using x-ray technique, Robins et al. concluded that, regarding the orientation of the fibres, no significant difference could be found between the vibrated and the sprayed beams. However, for both methods, the fibres tended to align in a partially random 2D plane at right angles to the direction of casting or spraying. Looking at the fibre density distribution, they noted that, for the vibrated concrete at a fibre-volume fraction of $V_f = 1.0\%$, the concentration of fibres at the bottom of the beams was approximately four times higher than at the top. For the sprayed beams, they found a more even distribution over the beam height, although with a slight

reduction at the bottom; they related this reduction to fibre rebound in the initial layers. Fibre distribution in the longitudinal direction was only briefly mentioned. The large difference in distribution over the height for the cast specimens, and to some extent for the sprayed specimens, can be overcome by using self-compacting concrete (SCC). The rheology of the fresh concrete is changed in SCC so that it is capable of filling the mould without vibration, and the cement paste is capable of filling all the voids between fibres and aggregates, Grünewald (2004). However, unless techniques similar to SIFCON or SIMCON are used, the fibre distribution, in terms of both orientation and density, cannot be fully controlled. Dössland (2008) investigated the fibre distribution of self-compacting fibre reinforced concrete in one wall and one slab element of a size of $4 \cdot 2.5 \cdot 0.15\text{m}^3$ and $2 \cdot 3 \cdot 0.2\text{m}^3$, respectively. The concrete was poured from one side of the formwork. To investigate the fibre distribution, 12 beams (6 in the longitudinal and 6 in the horizontal direction) were cut from the wall and six beams in were cut from the slab element in the longitudinal direction, all tested in bending. The residual strength was determined according to the Norwegian design draft proposed by Thorenfeldt, Sandaker et al. (2006). No difference was found between the horizontally and the longitudinally cut beams for the wall series, although the scatter for this series was relatively large; the scatter was smaller for the slab. A second investigation of the effect of casting method on the fibre distribution was also conducted. Wall 1 was cast by moving the nozzle back and forth over half the length of the formwork during casting; wall type 2 was cast with the nozzle held still at one end of the formwork. Beams were cut from the wall elements, again tested in bending. It was found that the average residual strength decreased with the flow distance in all beams; moreover, the residual strength was higher for the beams cut from the wall produced with the nozzle moving over half the length of the formwork during casting. Hence, the casting method plays a major role in the fibre distribution.

3 Experimental programmes

Two separate experimental programmes were carried out in the project. The first, which concerned splitting and bending, included material characterization by Wedge-Splitting Tests (WST) in cubic specimens and 4-Point Beam Bending Tests (4-PBT) in full-scale beams, see Paper II and Section 5. Investigating the flexural behaviour and determining what was need for further work on small crack widths may be considered as a preliminary study; this is listed in Table 3.1.

It was found in the study of splitting and bending that, for small cracks, it is necessary to be quite particular about the properties of the interface between the concrete and rebar. The bond stress-slip relationship thus needs to be accurately determined. Furthermore, the stress-crack opening (σ - w) relationship needs to be known in detail; other investigations have concluded that this relationship has a strong influence on the flexural behaviour, e.g. Zhang and Stang (1998). A bending test involves different phenomena and is much more complex with regard to cracking than a direct tension test. In real structures, flexural or shear loading (or a combination of both) is more common than direct tension; still, to better understand the cracking process, it was decided to carry out tension tests on prismatic specimens, also known as tie elements (Paper III). In direct tension, the size effect is eliminated and the cracking occurs in a purer manner.

The WST, used in the preliminary study to obtain properties for the σ - w relationship, does not directly provide the σ - w relationship. However, an approximate relationship can be obtained by inverse analysis, which is more closely described in Section 4. Since the inverse analysis does not yield one unique solution, it was decided to conduct uniaxial tensile tests (UTT) for the detailed study of tension and pull-out, see Paper III.

A study of the literature revealed that contradictory findings have been reported regarding the effect of fibre reinforcement on the bond stress-slip relationship. It was consequently decided to carry out pull-out tests with a short embedment length. It was possible in this way to determine the actual bond-slip properties for the materials tested here. Furthermore, the experiments were modelled in 2D in the preliminary study. Hence, it was not possible to consider the effects of the radial deformation when modelling the interaction between the concrete and the rebar. If instead a 3D model was used, it would be possible to study the effects in all directions in detail. This could be achieved using the 3D bond model developed by Lundgren (2005), see Paper IV.

Thus the second testing programme, the study of tension and bond, covered tie element tests, UTT, and pull-out tests with a short embedment length, see Papers III – V and Section 6. The test programme is listed in Table 3.2, and a principal explanation of the second study is shown in Figure 3.1.

Both testing programmes encompassed self-compacting concrete, reinforced with 35mm-long, end-hooked steel fibres, DramixTM RC 65/35-BN, supplied by Bekaert, Belgium.

Table 3.1 Experimental programme one, flexural cracking.

Series	Fibre content V_f [%] / [kg/m ³]	Rebar B500B No. ϕ [mm]	WST No.	Beams No.
1- V_f 0- ϕ 8	-	3 ϕ 8	9	3
2- V_f 05- ϕ 8	0.50 / 39.3	3 ϕ 8	9	3
3- V_f 025- ϕ 6	0.50 / 39.3	3 ϕ 6	9	3
4- V_f 05- ϕ 6	0.25 / 19.6	3 ϕ 6	9	3
5- V_f 075- ϕ 6	0.75 / 58.9	3 ϕ 6	9	3

Table 3.2 Experimental programme two, cracking due to tension.

Series	Fibre content V_f [%] / [kg/m ³]	Rebar B500BT ϕ [mm]	UTT No.	Pull-out No.	Tie element No.
0.0	0	16	5	5	5
0.25	0.25 / 20	16	6	5	5
0.5	0.50 / 40	16	6	5	5
1.0a	1.0 / 80	16	6	5	5
1.0b	1.0 / 80	16	6	5	5

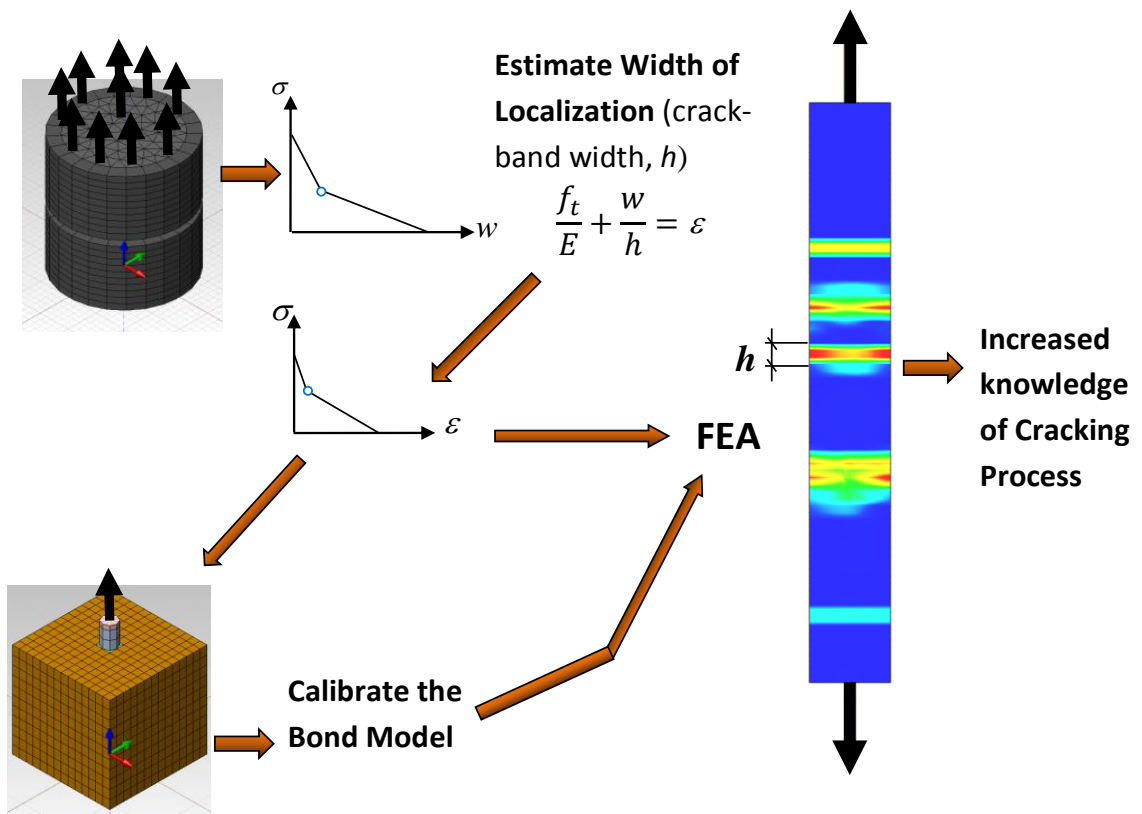


Figure 3.1 Principal explanation of the study of cracking due to tension.

4 Non-Linear Finite Element Modelling

All the laboratory tests except the UTT were analysed with non-linear finite element methods. The software used was Diana, release 9, developed by TNO Delft, see e.g. TNO (2011). Two-dimensional analyses were used in the study of splitting and bending, while 3D analyses were used in the study of pull-out and tension. The concrete in the models was assumed to be homogenous; this is usually an acceptable assumption for a strain-softening material. It was found that this assumption becomes inappropriate when the material has a high residual (post-cracking) tensile strength, however, i.e. when it exhibits a behaviour close to hardening, and is used in combination with a conventional reinforcement.

4.1 Tensile behaviour

A discrete crack model was used for the concrete in the analyses of the WST; a smeared, total strain, rotating crack model was used for the remaining analyses.

4.1.1 The tensile strength

The tensile strength may be obtained directly through uniaxial tension tests or indirectly on the basis of e.g. the compressive strength or a tensile splitting test. For the work described here, the tensile strengths used in the study of splitting and bending were obtained as a parameter in inverse analyses. For the study of tension and pull-out, they were obtained from tensile splitting tests; the tensile strengths obtained were compared with the ones measured directly in uniaxial tension tests on notched cylinders, see Section 6.1.

4.1.2 The softening curve

With the introduction of fibre reinforcement, the concrete matrix itself became able to withstand tensile loading, as the fibres could transfer stresses across the cracks. In this way, the part of the stress-displacement curve beyond the maximum stress became interesting. This residual behaviour could be strain hardening or strain softening, as described in Section 1.1, and can be obtained as the stress-crack width (σ - w) relationship. A straightforward method for obtaining the σ - w relationship is the uniaxial tension test, see Section 6.2. Unfortunately, the test set-up is cumbersome, and it is difficult to provide a sufficiently stiff testing equipment; thus this method is not widely used (Barragán (2002), Dupont (2003), Laranjeira de Oliveira (2010) and da Cunha (2010)).

The σ - w relationship can also be obtained indirectly by curve fitting, known as inverse analysis. The inverse analysis is based on results of a test method that does not yield the direct uniaxial relationship, e.g. beam-bending or wedge-splitting tests. In this case, while the σ - w relationship obtained is not unique, the method is still often preferred because of the simplicity of the test set-ups. Both direct tensile testing and inverse analyses were used for the work described here, but no comparison was made between the two regarding the applicability of the methods. The approach with inverse analysis was used in the study of splitting and bending, and the direct approach, performing UTT, was used in the study of pull-out and tension.

Indirect testing and inverse analysis

Starting from the splitting load-deformation ($F_{sp} - \delta$) curve from a wedge-splitting test (WST), or the load-deflection curve from a beam-bending test, the aim of the inverse analysis is to recreate the experimental curves as closely as possible. A numerical model of the test is created and the shape of a $\sigma-w$ relationship is estimated and used in analyses of the model. The shape of the $\sigma-w$ relationship is changed in a step-wise manner until the model yields a result close enough to the test curve.

Direct tension testing

In the study of cracking due to tension, uniaxial tension tests were carried out, see Section 6.2. As mentioned, this type of testing directly yields a unique solution for the $\sigma-w$ relationship. The $\sigma-w$ relationships obtained were used in analyses of the pull-out tests and the tie elements (Section 6).

4.1.3 Stress-strain ($\sigma-\varepsilon$) relationship

The cracks were modelled using the smeared crack approach. This means that the crack process zone should be “smeared out” over a distance - the crack-band width, h . This is not an objective parameter but depends on the size and shape of the selected mesh, Kooiman (2000). The smeared crack approach is based on the fictitious crack model (FCM) created by Hillerborg et al. (1976) and further developed for FRC by Hillerborg (1980). Up to peak stress, the tensile behaviour is represented by a pure $\sigma-\varepsilon$ relationship; once a crack forms, the fracture zone is assumed to be represented by the $\sigma-w$ curve, and the areas outside the fracture zone are related to the $\sigma-\varepsilon$ curve (Figure 4.1).

In the FE model, to be able to use the $\sigma-w$ relationships obtained, the crack widths must be translated into strain. The strains for the FE analyses were obtained as (TNO (2005)):

$$\varepsilon_i = \frac{f_t}{E_c} + \frac{w_i}{h} \quad (4.1)$$

where f_t and E_c are the tensile strength and Young's modulus of the matrix, respectively, w is the crack width measured from the UTT (or inverse analysis) and h is the crack band width.

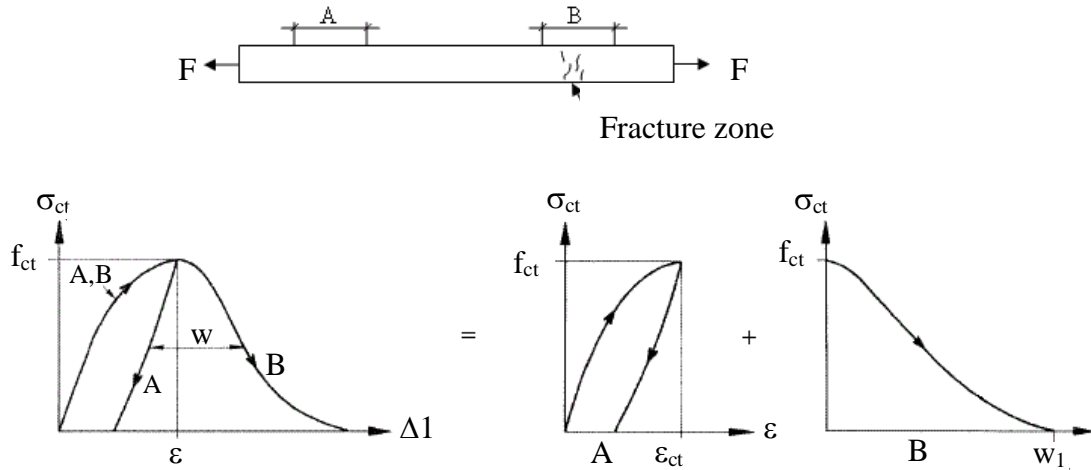


Figure 4.1 According to the FCM by Hillerborg, the tensile deformation can be divided into a strain part related to deformations outside the fracture zone and a crack part, w , which is the additional deformation due to the formation of a fracture zone; modified from Hillerborg (1983).

4.2 Compression curve and Young's modulus

For the study of splitting and bending, the compressive strength was tested on cubes with a side of 150mm. The elastic modulus was obtained from the inverse analyses of the WST.

In the study of tension and pull-out, the compressive strength and the elastic modulus were tested on cylinders with a diameter of 150 mm and a height of 300 mm. The compressive strength was tested according to the Swedish standard SIS - Bygg (2009). For the majority of the FE analyses, the complete compression curves of the concrete were assumed as suggested by Thorenfeldt, following the work of Popovic (1973). For the 4-PBT, a few analyses were run assuming an elastic-plastic compression curve; the Thorenfeldt curve was adopted for the remaining analyses.

4.3 Bond behaviour

The WST and the beam-bending tests were modelled in 2D for the study of splitting and bending; thus the interaction between rebar and concrete, the bond behaviour, can be described only in the longitudinal direction. A common assumption is that the reinforcement is embedded in the concrete; with this approach, it is assumed that all elements crack and it is only possible to study the overall behaviour in terms of e.g. load capacity. For the 4-PBT in the study of splitting and bending, slip was allowed between the rebar and the concrete. The interaction between the rebar and the concrete was described with an explicit bond stress-slip relationship. In this way, the cracks are expected to localize in a distinct crack pattern resembling reality, and both crack distance and crack opening may be studied. The relationship adopted was assigned to line interface elements between the concrete and the reinforcement bar and was in accordance with the suggestion for plain concrete in Model Code 90 (1999).

When the rebar slides in the concrete, irregularities on the steel surface (and/or the lugs) give rise to radial deformations, which in turn cause stresses directed outward at

an angle, α , and can cause longitudinal splitting cracks, see Figure 4.2. These stresses, known as inclined compressive stresses, are schematically shown in Figure 4.3. The explicit bond stress-slip relationship does not consider the radial deformations and their related stresses; thus, the splitting cracks induced by the inclined compressive stresses cannot be studied. It was decided to model the tests in 3D for the study of tension and pull-out. In this way it should be possible to consider stresses in all directions. To achieve this, however, a different bond model must be employed; the interaction between concrete and rebar was described with a special model, relating deformations with stresses. The bond model used, first formulated in Lundgren and Gylltoft (2000), and later modified in Lundgren (2005), is especially suited for 3D modelling, where the concrete and the reinforcement are modelled with solid elements. The interaction between concrete and steel is represented by surface interface elements, which, through the bond model, have been assigned properties regarding the relation between: the slip along the rebar, the normal displacement and the tractions in the normal and tangential directions.

The model is a frictional model, using elasto-plastic theory to describe the relations between the stresses and the deformations. Figure 4.3 shows the principle of the yield surfaces of the bond model. For details on the bond model, see Paper IV and Lundgren (2005).

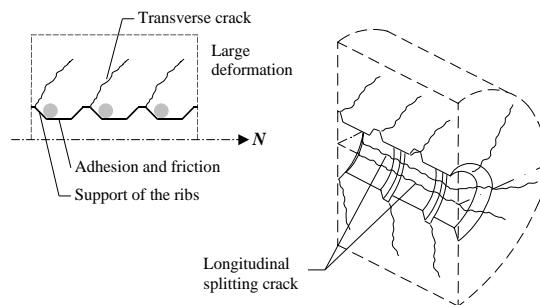


Figure 4.2 Deformation zones and cracking caused by bond, modified from Vandewalle (1992).

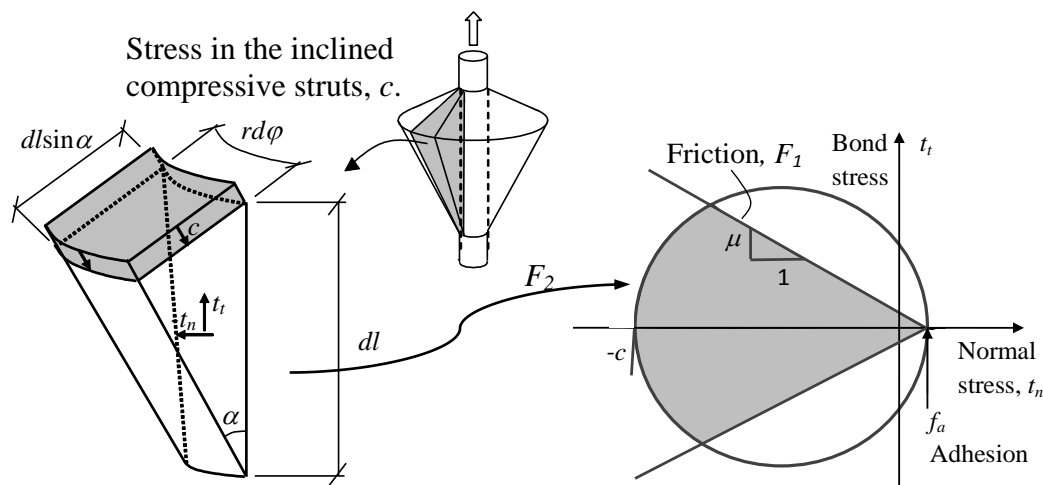


Figure 4.3 The yield surface, F_2 (upper limit at pull-out failure), and the limiting friction, F_1 , of the bond model, modified from Lundgren (2005).

5 Study of Splitting and Bending

The study of splitting and bending, encompassing WST and 4-point beam-bending tests, is reported in paper II. All the tests were conducted at the laboratory at Chalmers University of Technology.

5.1 Material properties

The compressive strength, f_{cm} , was obtained at 28 days on standard cubic specimens, while the tensile strength, f_{ct} , and the elastic modulus, E_{cm} , were parameters of the inverse analysis of the WST.

5.2 Wedge-splitting tests: Experiments

It is relatively easy to carry out a wedge-splitting test, and the test specimens are small and easy to handle. The WST was used to implicitly determine the stress-crack opening relationships of the materials tested in the study of splitting and bending. It is performed on a cast cubic specimen, here with a side of 150 mm, which is suitable for fibres of a length of ~ 30 mm; a larger specimen is required for longer fibres, see Löfgren et al. (2004). The test set-up and principle of the WST are shown in Figure 5.1. A wedging device is placed in the cast groove, and a vertical load is applied. Through the roller bearings on the steel-loading device, the vertical load is transformed into the horizontal splitting load, F_{sp} , which forces the two sides of the cube apart. The vertical load applied, F_v , is related to the splitting load as:

$$F_{sp} \approx \frac{F_v}{2 \tan(\alpha)} \quad (5.1)$$

where α is the angle of the wedge, here $\alpha = 15^\circ$. To ensure stable crack propagation in the plane, a 53-mm deep starter notch was cut lengthwise in the centre of the cast groove; in addition, a 25-mm deep guide notch was cut on the edges of the crack plane, see Figure 5.1 and Figure 5.2. The average results in the form of load-CMOD curves from the experimental wedge-splitting tests are shown in Figure 5.3.

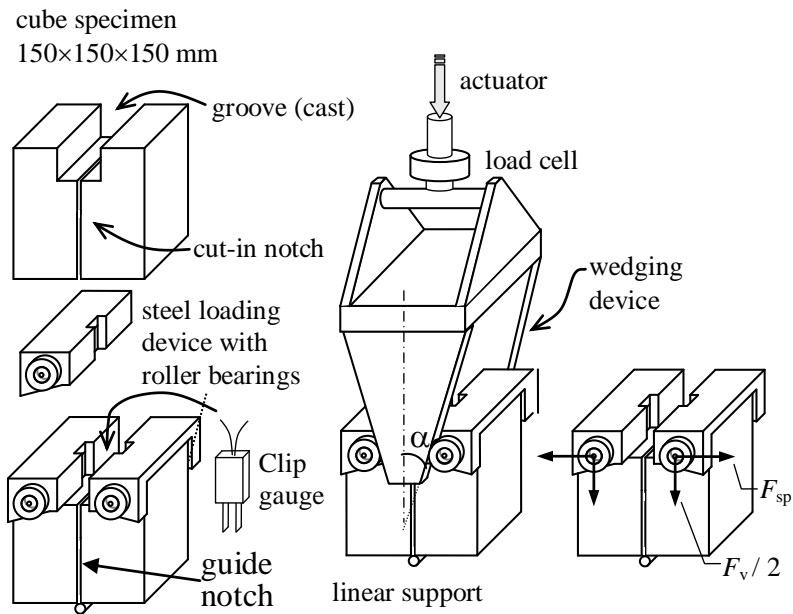


Figure 5.1 Principle of the wedge-splitting test method, from Löfgren (2005).

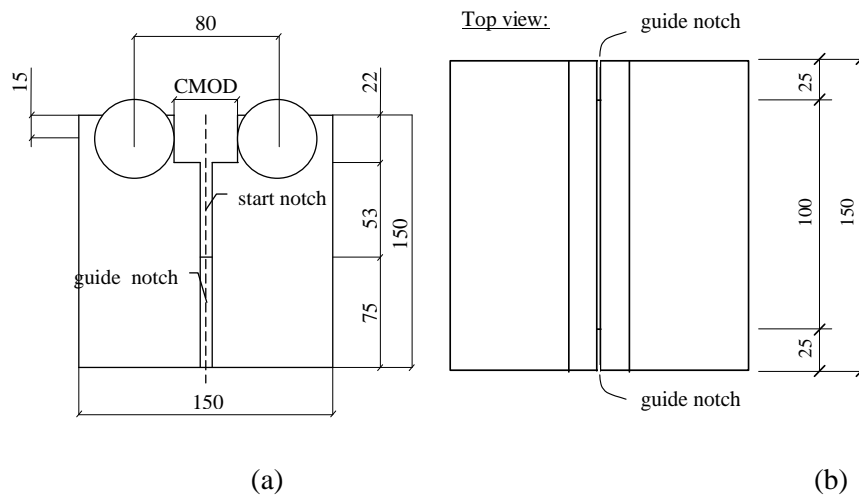


Figure 5.2 Distance between the roller bearings, and dimensions of the notches, modified from Gustafsson and Karlsson (2006).

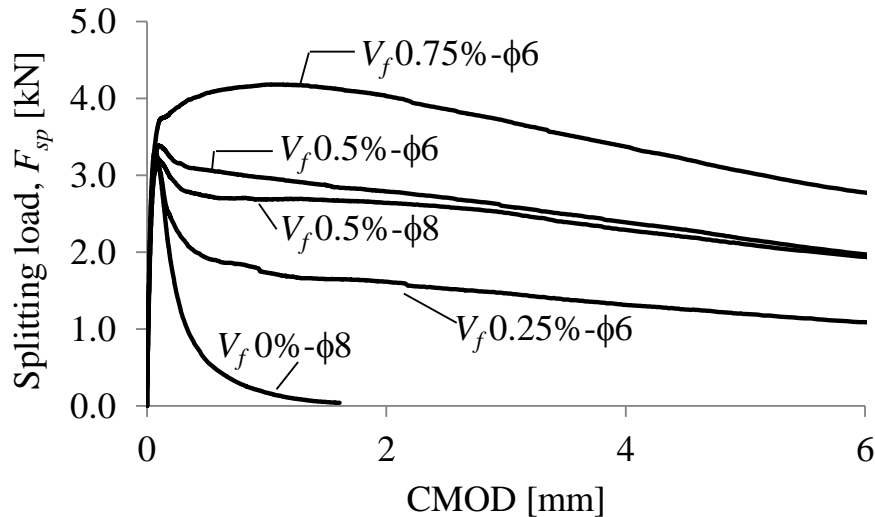


Figure 5.3 Average WST results for each series.

5.3 Wedge-splitting tests: Non-linear analysis

The purpose of the WST analyses was to obtain the uniaxial stress-crack width ($\sigma-w$) relationships for the materials in testing programme one. Since the crack in a WST opens in a manner that resembles bending rather than uniaxial tension, the results can not be used directly. Instead, by assuming different $\sigma-w$ relationships, the WST was simulated with FEA. This approach is known as inverse analysis (Section 4.1).

The WST cube was modelled in half (symmetry) using the discrete crack approach (Figure 5.4). No characteristic length (crack-band width) is needed with this approach since the crack is predetermined to occur exactly in the elements along the symmetry line.

In reality, the horizontal splitting load is achieved from the applied vertical load, which is transformed into horizontal loading through the roller bearings. In the inverse analysis, however, both the vertical and the horizontal loads must be applied in the loading point (Figure 5.4). The horizontal component was obtained by using Equation 4.1, and the two forces were applied through stepwise incrementation. The fracture energy, G_F , which is a major factor in fracture mechanics, is kept the same in the FE analysis as it is in the WST experiments by the agreement of the two resulting load-CMOD curves in the present case.

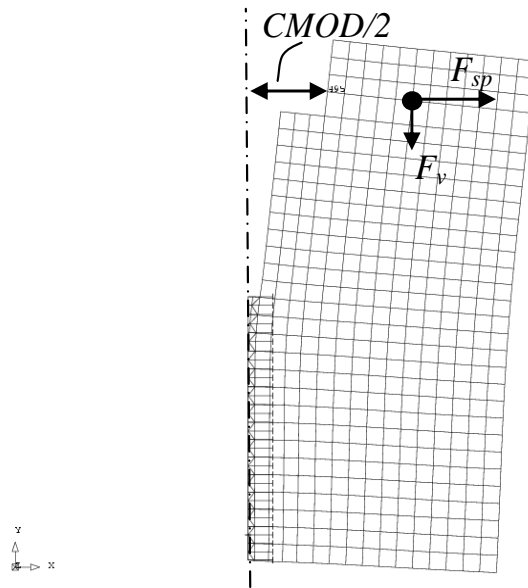


Figure 5.4 FE model of the WST specimen.

Starting from the load-deformation ($F_{sp} - \delta$) curve from the wedge-splitting test (WST), the inverse analysis was performed as a stepwise iteration. The WST was simulated with non-linear, finite-element analysis (FEA), adopting different shapes of a $\sigma-w$ curve until the result gave a satisfactory agreement with the experiments. The $F_{sp} - \delta$ curve from the analysis was compared with the experimental one by checking the splitting load ratio $F_{sp.inv} / F_{sp.exp}$ at multiple locations. When this ratio was within a range of 0.95 – 1.05 (i.e. when Δy_i in Figure 5.5 was small enough), the inverse analysis was considered to be completed. Two types of $\sigma-w$ relationships were evaluated: a bi-linear and a multi-linear relationship, see Figure 5.6. The procedure of the inverse analysis is further described in Paper II.

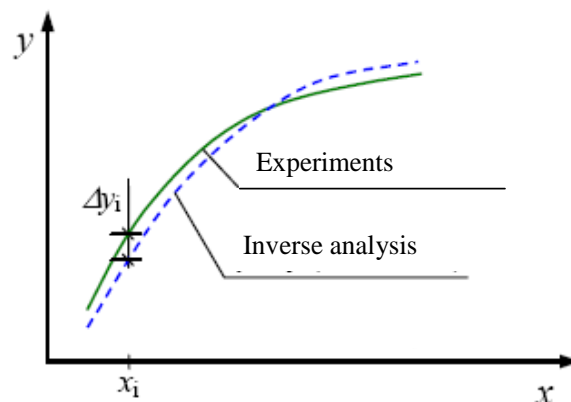


Figure 5.5 Schematic of the principle of the inverse analysis.

An example of the final result of the inverse analysis using a multi-linear $\sigma-w$ relationship for the series with a fibre amount of $V_f = 0.75\%$ is shown in Figure 5.7. It is seen that the agreement between the experiment and the analysis is very good; this is quantified in Figure 5.8, where the splitting load ratios between experiments and analyses are shown for all of the series. The reason for the less good agreement when a bi-linear approach is used is found in the fewer number of points representing the $\sigma-w$ curve, compared with the multi-linear approach. The $\sigma-w$ relationships from the

inverse analyses were used in the FEA of the 4-point beam bending tests (Section 5.5). Although the multi-linear relationship yielded markedly better agreement with the experimental WST results (Figure 5.8), it was seen in the FEA of the 4-point beam bending tests that, for load bearing purposes, the bi-linear and multi-linear σ - w relationships yielded equally good results.

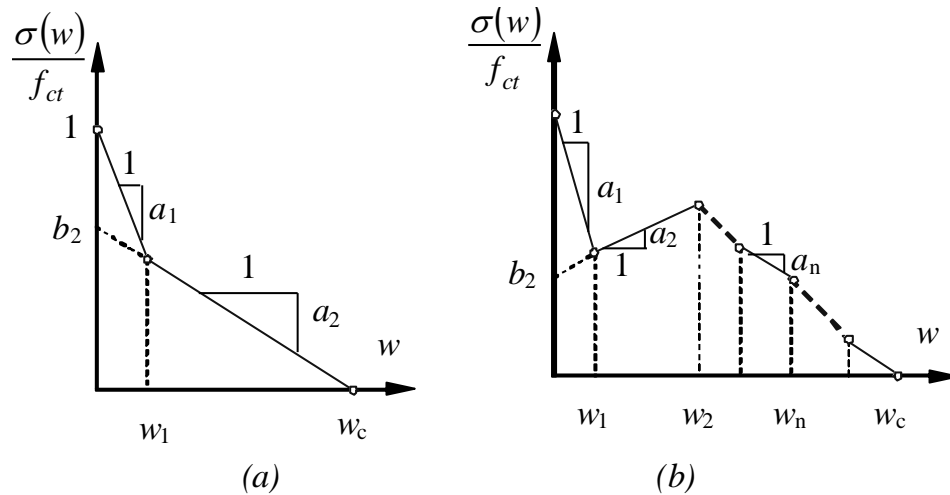


Figure 5.6 General shape of the two types of simplified stress-crack opening relationships used for the FE analyses: a) bi-linear and b) multi-linear.

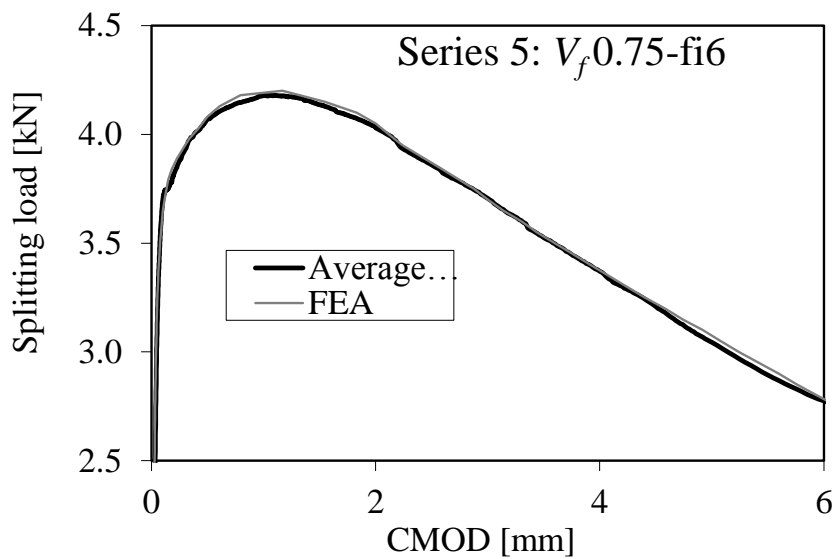


Figure 5.7 Inverse analysis of the multi linear σ - w relationships, here for the series with $V_f = 0.75\%$ (the difference between the curves is barely noticeable).

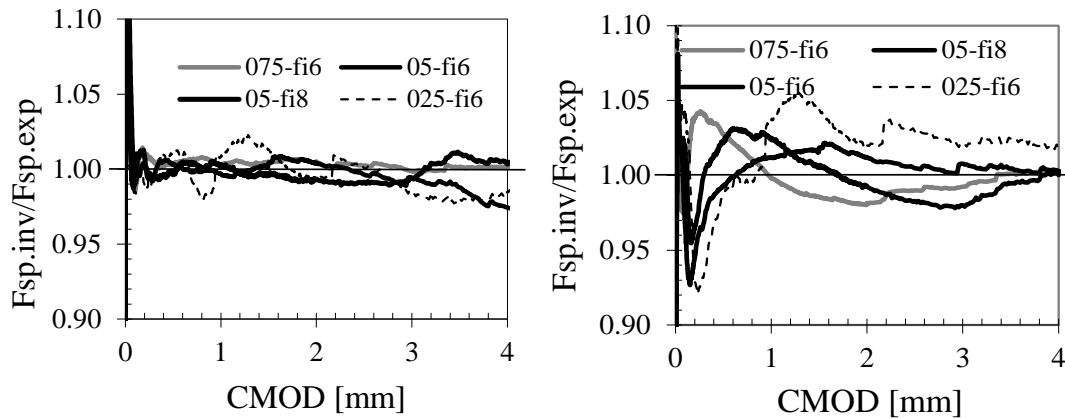


Figure 5.8 Comparison of inverse results with experiments through ratio F_{FE}/F_{exp} : (a) using multi-linear σ - w curves and (b) using bi-linear.

5.4 4-point beam bending: Experiments

Full-scale tests of beams in bending were carried out to investigate the flexural behaviour of steel fibre-reinforced concrete, see Figure 5.9. The varying variables were the fibre-volume fraction V_f , and the diameter of the reinforcement bars. The results of the tests and comparisons with finite element analyses are presented in Paper II; more details can be found in Gustafsson and Karlsson (2006). The beams were designed for moment failure, and this was the failure mode achieved. Figure 5.9 and Figure 5.10 show the test set-up and dimensions. During testing, several bending cracks developed within the area of “constant” moment and also shear-bending cracks outside this area. At failure, only one crack was still active. This can be seen in Figure 5.11, which shows a photo of the cracks in one of the tested beams. The crack spacing varied depending on the amount of fibres added; as expected, there was a decrease in crack spacing for an increasing amount of fibre. Figure 5.12 shows the load-deflection results for one of the tested series.



Figure 5.9 Set-up for the beam-bending tests, from Gustavsson and Karlsson (2006).

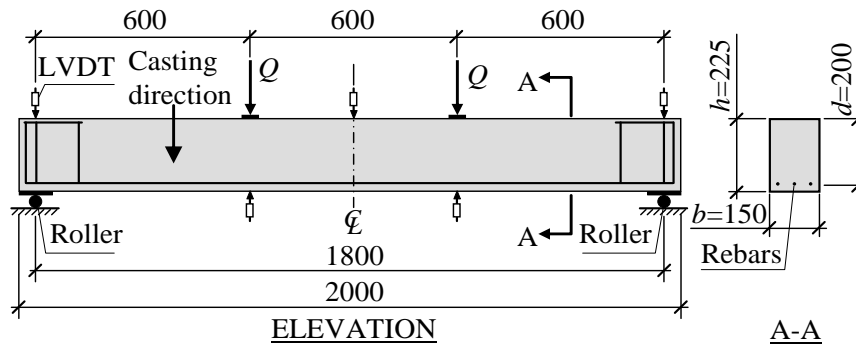


Figure 5.10 Dimensions and loading conditions.

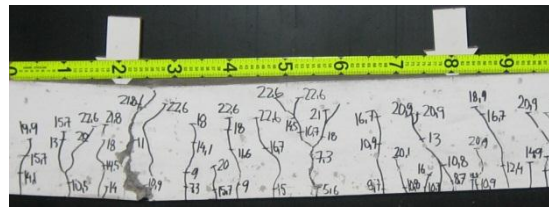


Figure 5.11 Crack pattern in one of the beams from Series 5: $V_f 0.75\text{-fi6}$.

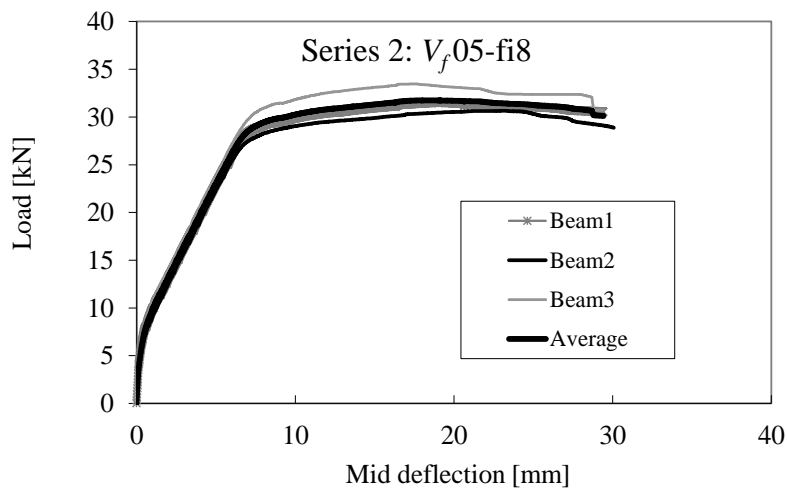


Figure 5.12 Load-deflection curves for the three beams in Series 2 with a fibre content of $V_f = 0.5\%$ and rebar diameter $\phi = 8\text{mm}$.

5.5 4-point beam bending: Non-linear analysis

The beams tested were modelled in 2D, using plane-stress solid elements for the concrete, with a mesh-element size of $5 \times 5\text{mm}^2$, (Figure 5.13). This type of element has four integration points and is based on linear interpolation and Gauss integration. The reinforcement was modelled using truss elements; this type of element can deform only in the axial direction. The interaction between rebar and concrete was modelled with interface elements given bond-slip properties according to the bond model suggested by Model Code 90 (1999), assuming a confined situation with good bond conditions. The tensile-softening behaviour (stress-crack width ($\sigma\text{-}w$) relationship) of the concrete was obtained through inverse analysis of wedge-splitting

tests, see Section 5.3. One purpose of the work was to investigate whether a multi-linear σ - w relationship could better describe the cracking process in flexural beams as compared to a bi-linear σ - w relationship.

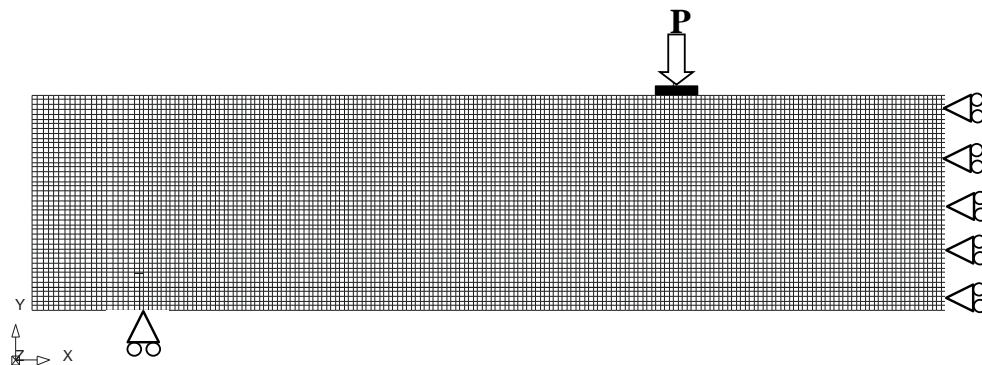


Figure 5.13 The 2D mesh used for the beam analysis.

It was observed when studying the results that, for the overall behaviour, in terms of load-deflection curves and maximum loads, both relationships show equal agreement with the experimental results. Looking at the average crack spacing, there were indications that the analyses using multi-linear σ - w relationships could better capture the trend with decreasing crack spacing for increasing fibre-volume fractions, see Figure 5.14, where a comparison is made between the beam-bending tests, the FEA, an analytical model by Löfgren (2007), a proposal by RILEM (2003), and the new Model Code (2010). A comparison of the experimental and the analytical crack patterns for Series 2 is shown in Figure 5.15. The calculations for average crack spacing, s_{rm} , based on MC2010, were carried out by Master students Abid and Franzen (2011). It is seen in Figure 5.14 that the calculation with the suggestion in Model Code 2010 seems to predict smaller crack spacing as compared with the experimental results. This might be because the assumed mean value for the bond stress between steel and concrete, $\tau_{bm} = 1.8 \cdot f_{ctm}$ is too high. Furthermore, in the calculation of the crack width, the coefficient β , which is used to determine the mean strain over the length at which slip occurs, is assumed to be the same for FRC as for plain concrete. This does not agree with the findings in Paper III and in Bischoff (2003), where it is clearly seen that β increases with an increasing fibre content.

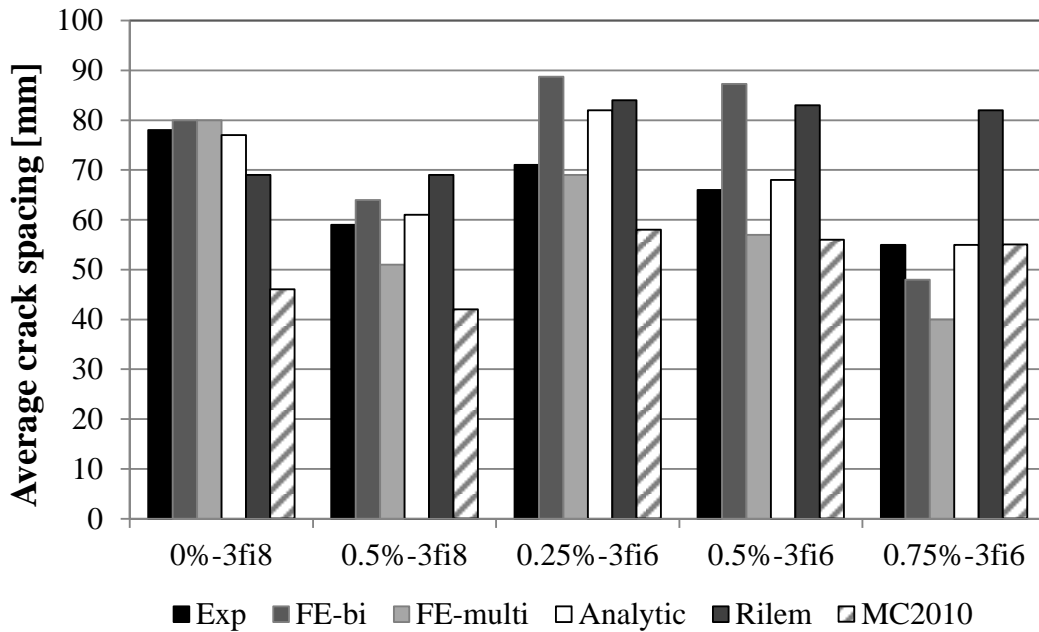


Figure 5.14 Comparison between calculated crack spacing and the crack spacing obtained in the experiments.

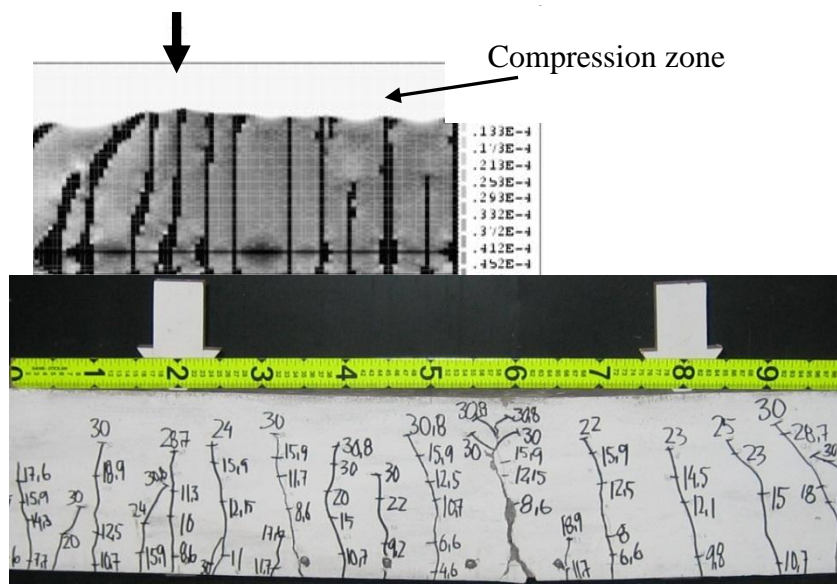


Figure 5.15 Comparison of the FE result for series 2:0.5%-fi8, multi-linear σ -w with crack band width, $h = 60\text{mm}$. Photo from Gustafsson and Karlsson (2006).

6 Study of Tension and Bond

The second study covered tension and pull-out tests, and numerical analyses of the same. The tension tests included uniaxial tension tests (UTT) of cylinders and tension tests of prismatic concrete members known as tie elements. The test set-up for the UTT is quite cumbersome, as mentioned in Section 4.1; investigating the possibilities of conducting the UTT at a different location, it was found that the possibilities for this were limited. Instead, together with the Technical Research Institute of Sweden (SP), a testing rig was developed that fulfils the RILEM (2001) requirements, and the UTT was carried out satisfactorily. Paper III treats the experimental part of the tension tests. The second study also included pull-out tests with a short embedment length. These tests, together with the tie element tests, were carried out at the laboratory at Chalmers University of Technology. Paper IV covers both testing and analysis of the pull-out tests, while Paper V solely treats the analyses of the tie elements.

6.1 Material properties

In the second study, the compressive strength, f_{cm} , was determined on cylinders at 28 days of age. The elastic modulus, E_{cm} , was also determined on cylinders; however, owing to some complications with the test equipment, the elastic modulus was tested at age 300 days at CBI, Stockholm. The values of E_{cm} needed for analysis at different specimen ages were determined through formulas for time dependency, found in EC2 (2004). The (splitting) tensile strength, $f_{ctm,28d}$, was determined after 28 days on water-cured cubes $150 \times 150 \times 150 \text{ mm}^3$ following the Swedish standard SS-EN 12 390-6. The tensile strength was obtained as:

$$f_{ctm} = 0.7 \cdot f_{ctm.sp.28d} \quad (6.1)$$

Generally, it is not recommended to determine the direct tensile strength from a uniaxial tension test on a specimen with a cut notch along the perimeter, e.g. RILEM (2001). Nevertheless, when comparing the direct tensile strengths obtained from equation (6.1) with the cracking stresses from the UTT, it was seen that they agreed quite well, see Table 6.1. The UTT was carried out at a specimen age of 165 days. Thus, to compare the tensile strength derived from the splitting test with the maximum stress from the UTT, the increase in strength over time $t = 165$ days was considered according to EC2 (2004) to be:

$$f_{ctm}(165d) = \beta(t)^{2/3} \cdot f_{ctm} = 1.125^{2/3} \cdot f_{ctm} = 1.08 \cdot f_{ctm} \quad (6.2)$$

with;

$$\beta(t) = \exp \left[s \left[1 - \left(\frac{28}{t} \right)^{0.5} \right] \right] \quad (6.3)$$

in which s depends on the type of cement. For the cement used in the tests, CEM 42,5R, $s = 0.2$.

Table 6.1 Comparing tensile strength obtained with different methods.

Series	$f_{ctm.sp.28d}$ [MPa]	$f_{ctm.28d}$ [MPa]	$f_{ctm.165d}$ [MPa]	$f_{ctm.UTT}$ [MPa]
0.0	4.1	2.9	3.1	3.1
0.25	3.9	2.7	2.9	2.9
0.5	4.3	3.0	3.3	3.2
1.0a	4.8	3.4	3.7	3.6
1.0b	4.3	3.0	3.3	3.6

6.2 Uniaxial Tension Tests

Paper III reports the uniaxial tension tests (UTT) on cylindrical specimens, which were carried out at SP, the Technical Research Institute of Sweden, at a specimen age of 165 days. The alignment of the fibres affects the capacity, especially in tension. Thus, if a small specimen is manufactured by merely producing a mould of the same size as the final test specimen, due to the wall effect, the fibres will be aligned favourably, and the result will be misleading. To avoid this, the cylinders were cored from larger specimens.

The test set-up must be stiff enough to prevent rotation of the crack surfaces, i.e. to minimize the introduction of bending. Figure 6.1 shows a photo of the test set-up. According to RILEM (2001), the requirement for stiffness is fulfilled if, at the end of the test, the maximum difference between the individual transducer signals is less than 10% of the average displacement. This was achieved for all cases of the tested series. Figure 6.2 shows the average test results.

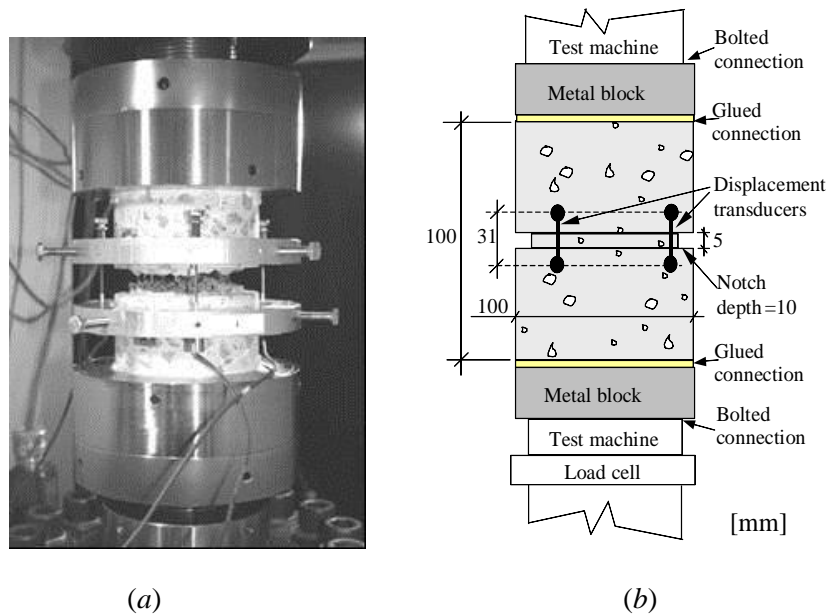


Figure 6.1 (a) Photo of the test set-up and (b) schematic of the same.

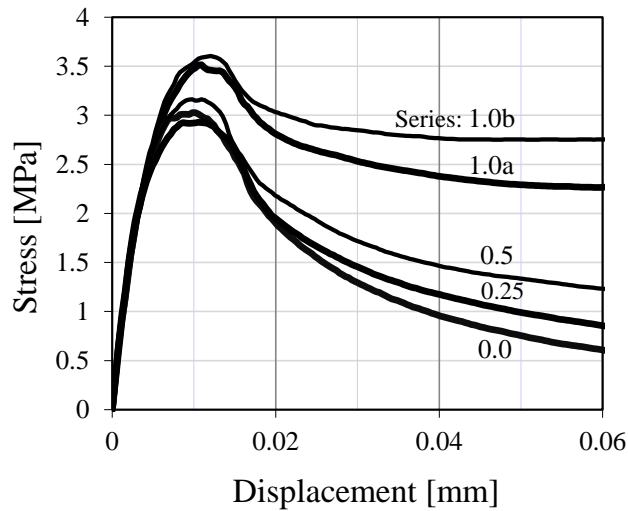


Figure 6.2 Average σ - δ curve for each tested series.

6.3 UTT analysis

The results obtained from the UTT are on the form of the load-displacement over the notch. To obtain the tensile stress, the measured load is simply divided by the area at the notch. The crack width, w_i , for each load step is obtained as the deformation that remains after the elastic deformation has been deducted (Equation 6.4), both in accordance with RILEM (2001).

$$w_i = \bar{\delta}_i - \bar{\delta}_{peak} \quad (6.4)$$

$\bar{\delta}_{peak}$ is the average deformation at average peak stress, and $\bar{\delta}_i$ is the average deformation across the notch, see Figure 6.3. Figure 6.4 shows the average σ - w curves for all series.

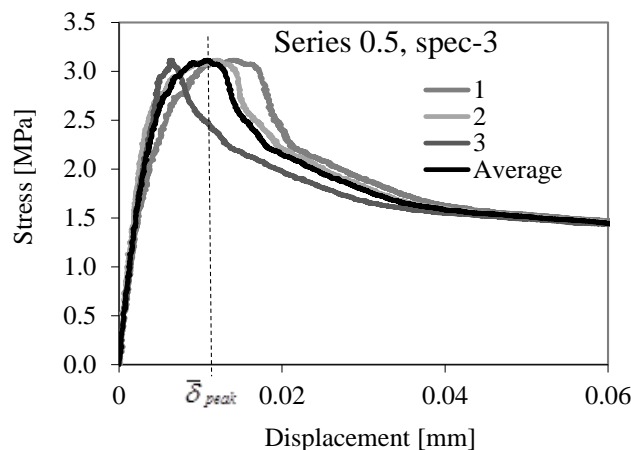


Figure 6.3 Example of the stress-displacement curves from one of the specimens in Series 0.5 and definition of $\bar{\delta}_{peak}$.

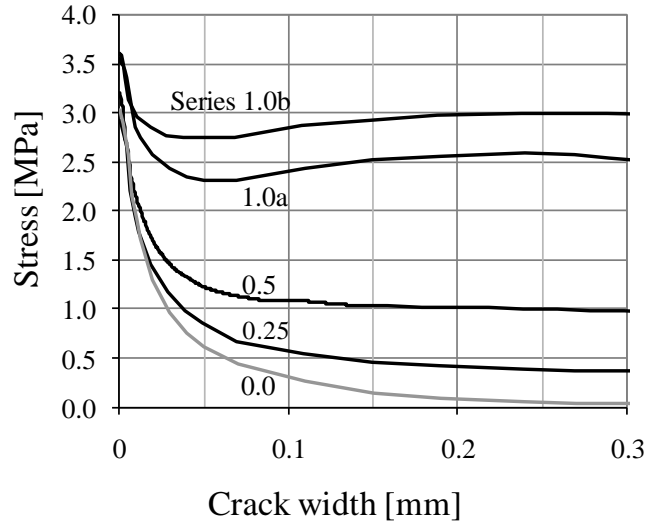


Figure 6.4 The average σ - w curves for each of the tested series.

6.4 Pull-Out Test with short Embedment Length: Experiments

The bond stress-slip relationship of the interface between the concrete and the reinforcement bar was investigated in pull-out tests, described in Paper IV. When we decided on the size of the test specimens, the idea was to choose a size with as small enough cover so that the surface strains would be measurable. At the same time, it was interesting to avoid splitting failure as long as possible in the specimens without fibre reinforcement. A third factor that was considered was the possibility of cracks reaching the surface in the tie element tests (Section). Preliminary tests were carried out for the pull-out and the tie elements, and it was seen that a maximum cover of 3ϕ could be used if a meaningful number of cracks were to reach the surface in the tie elements. For this cover, the pull-out tests for 0% fibre reinforcement proved to be able to reach the same magnitude of peak stress that was found in the fibre-reinforced specimens. A concrete cover of $3\phi = 48\text{mm}$ was thus adopted. To avoid an unwanted alignment of the fibres from the walls of the moulds, the specimens were cut from larger bodies. The specimen age at testing was 95 days.

In a structural member, the bond stress along the reinforcing bar varies along the length. However, in the test, if the embedded length of the rebar is made short, it is commonly assumed that the bond stress is evenly distributed. It may then be calculated as the measured force divided by the embedded surface area as:

$$\tau_{average} \approx \frac{F}{l_b \cdot \pi \cdot \phi} \quad (6.5)$$

where l_b is the embedded length and ϕ is the diameter of the rebar.

In the tests, the measured parameters were: the load-slip curve, and the radial, surface strains at one location on each of the four specimen sides.

As expected, the series without fibres failed in splitting (Series 0.0). The failure modes for the fibre-reinforced series changed with increasing fibre content from splitting induced pull-out, to pure pull-out failure. The scatter between the tested specimens within a series can be considered to be moderate, see Figure 10 in Paper IV, where the full results are shown. Figure 6.5 shows the geometry and test set-up,

and Figure 6.6 shows the average curves before peak stress for each series. In comparison, it is seen that Series 1.0b shows a lower stiffness and a lower peak stress. This is eliminated though if the bond stress is normalized with the compressive strength, see Figure 6.6b.

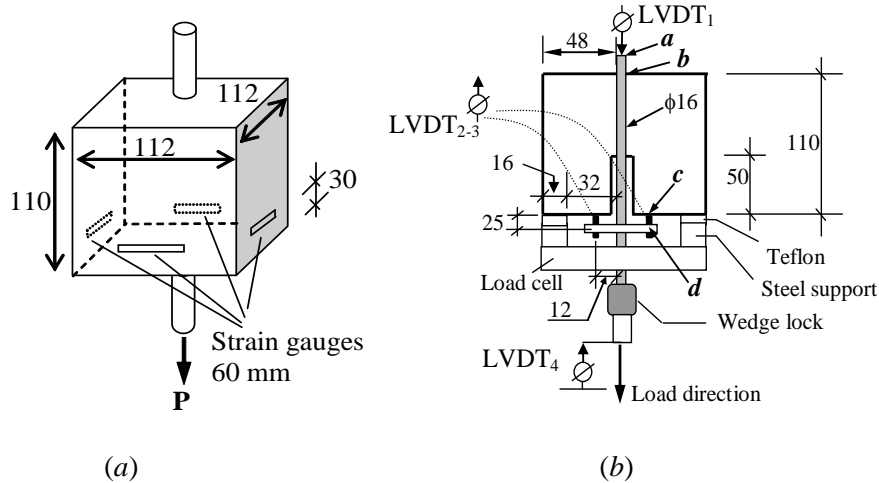


Figure 6.5 Geometry (a) and schematic view of the test set-up (b).

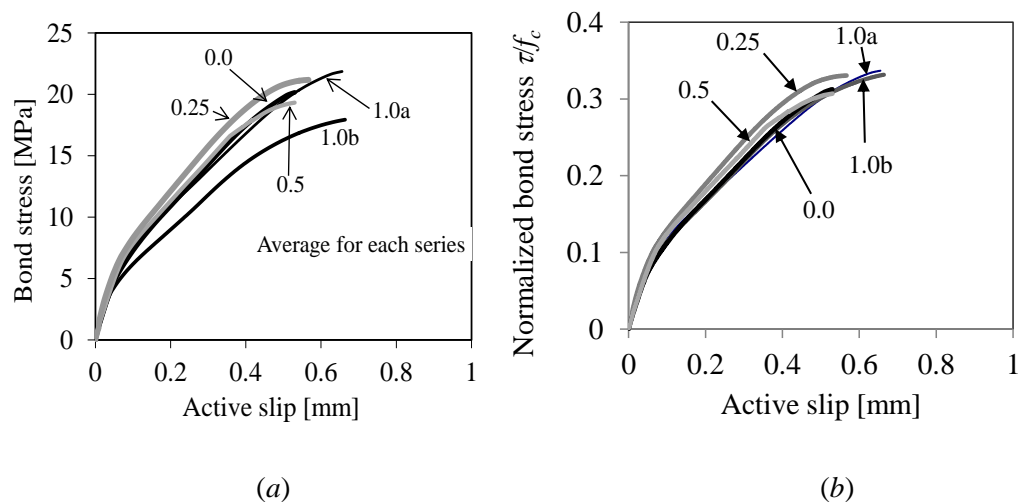


Figure 6.6 The average result before peak stress for each series; (a) bond stress-slip and (b) bond stress normalized with compressive strength-slip. See Paper IV for the residual part of the results.

6.5 Pull-Out Test with short Embedment Length: Non-Linear Analysis

Paper IV treats the analyses of the pull-out tests. In the analysis, it is possible to describe the interaction between the concrete and the rebar by the bond stress-slip relationship obtained from the pull-out tests. However, this relationship only provides the bond properties in the longitudinal direction. To be able to account for also the radial movement, and stresses occurring from this, a bond model, first formulated in Lundgren and Gylltoft (2000), and later developed by Lundgren (2005), was used, see Section 4.3. The bond model was originally calibrated for normal strength concrete,

vibrated, without fibres and rebar K500ST with diameter $\phi = 16\text{mm}$. This calibration was aimed for anchorage failure, thus larger slip values than considered here were of interest. When using the originally calibrated values, it was seen that the initial stiffness was too weak and the maximum stress was markedly overestimated (Figure 6.7), thus the model was re-calibrated to fit the results from the pull-out tests.

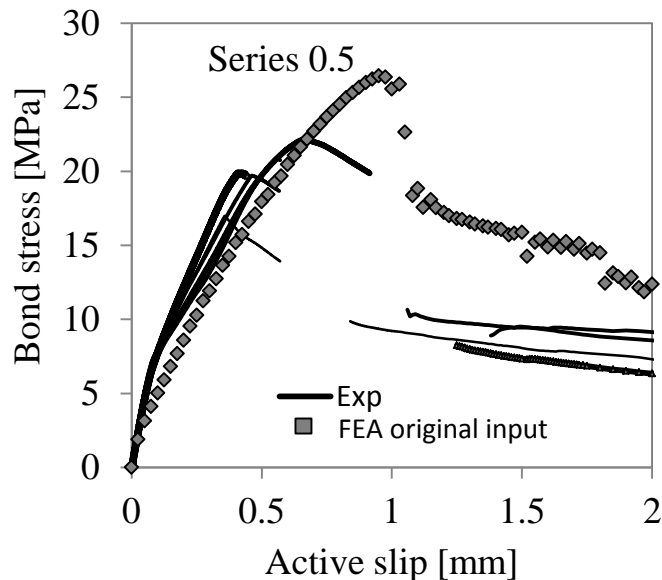


Figure 6.7 Analysis result using the original calibration on Series 0.5.

Studying the analyses it was seen that the cracking starts from two separate actions. The cracking induced by the inclined compressive struts, starts from the rebar and travels outwards as the slip increases. The other one is seen on the loaded (active) side of the specimen. Here a diagonal crack pattern becomes visible, resembling the envelope type of cracking, developing in a simply supported slab in yield-line theory. These cracks start from the outside. When the maximum stress is reached, the cracks from the first action take over, and for Series 0.0 the failure mode is splitting, see Figure 6.8. For Series 0.25 and 0.5 it is seen in the analyses, that after peak load, one of the cracks becomes more strained than the remaining three, but still there is a considerable residual capacity; this is seen in Figure 6.9, where results for Series 0.5 are shown. Due to this it seems incorrect to consider this a splitting failure. Instead a combined failure mode formulated by Magnusson (2000), was adopted; splitting induced pull-out failure. For Series 1.0a and 1.0b, the cracks keep open symmetrically around the specimen, and the specimens fail in pull-out, see Figure 6.10. Figure 6., which shows results for Series 1.0b. When studying the pull-out test specimens after testing it was noted that in two of the specimens from Series 1.0b there were no cracks visible to the naked eye and when using a crack microscope, the ones detected were of the size 0.005mm. These findings are reflected in the experimental load-deformation curves seen in Figure 6., where these two specimens did not experience the load drop that was seen in the remaining specimens (i.e. pure pull-out).

In the analyses, one difference between Series 0.0-0.5 and 1.0a-b is that the cracks don't appear on the passive side for Series 1.0a and 1.0b. This is due to the larger amount of fibres in Series 1.0a-b, which more effectively arrests the crack propagation, and consequently leads to a different failure mode.

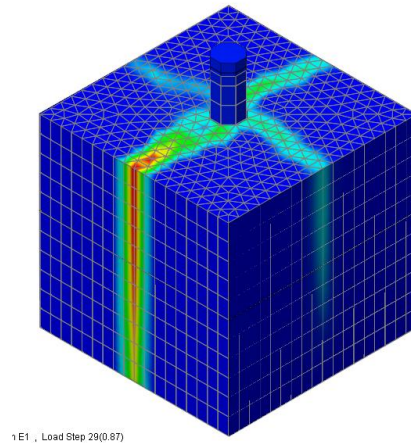


Figure 6.8 Series 0.0 - principal strain E1 for $h = 6.2\text{mm}$, applied deformation = 0.87mm .

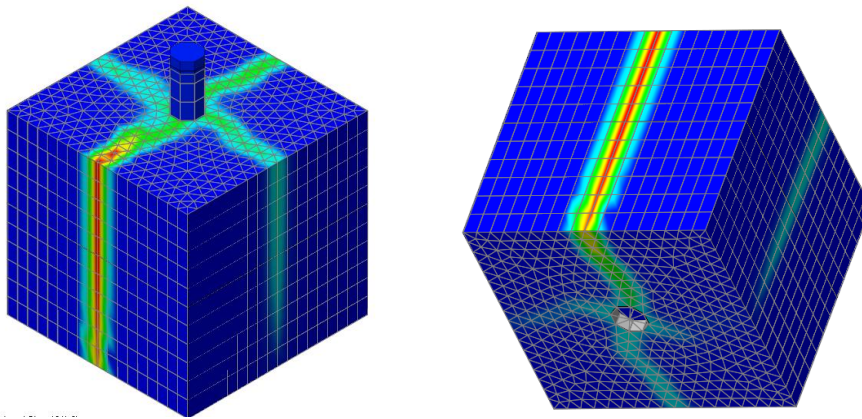


Figure 6.9 Series 0.5 - principal strain E1 for $h = 6.2\text{mm}$, applied deformation = 1.2mm .

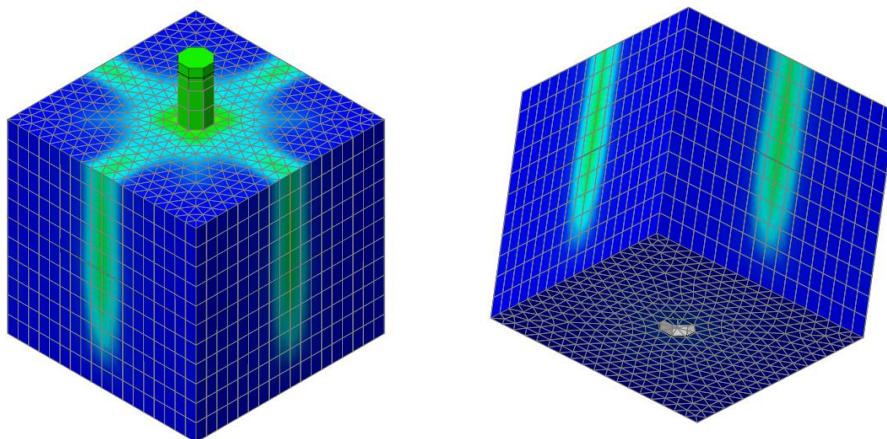


Figure 6.10 Series 1.0b - principal strain E1 for $h = 6.2\text{mm}$, applied deformation = 1.2mm .

Judging from the test results, the used fibres did not affect the bond properties before the maximum load; after that they provided increasing confinement for increasing fibre content. Instead there were indications that due to the self-compacting properties, the initial bond stiffness was increased. It may be explained by the increased amount of finer particles in the self-compacting concrete. This makes for a denser matrix, which easier fills out voids around the rebar; thus the bond may initially be stiffer than what is found for conventional vibrated concrete.

6.6 Tie Element Testing: Experiments

To study direct tensile cracking, tie element tests were carried out; these are treated in Paper III. Parallel with the usually measured load-deformation, on one surface of each specimen, the strain development was monitored by sequential photographing. This full-field strain measurement was performed on all tie elements tested in this study. The non-contact optical deformation measurement system ARAMISTM 4M by GOM, which relies on a measurement technique based on Digital Image Correlation (DIC), was used. The basic idea of DIC is to measure the displacement of the specimen during testing, by tracking the deformation of a speckle pattern on the surface, in a series of digital images acquired during the loading. This is done by analyzing the displacement of the pattern within discretized pixel subsets or facet elements of the image.

With the size of the monitored surface = 112mm x 500mm, the DIC technique used on the tie elements had an accuracy of ± 0.01 mm. Similar to the findings by Robins et al. (2001), the deformations could not be followed in detail before reaching a certain value, $w_{initial}$. The largest value that was detected in one of the specimens without fibres, was $w_{initial} = 0.21$ mm. This is due to the sudden opening of the cracks, which occurred momentarily to the value, $w_{initial}$, due to elastic unloading. It differed between the tested specimens but was markedly smaller for the SFRC series with fibre amount $V_f \geq 0.5\%$; with average $w_{initial} = 0.09$ mm, see Paper III. For geometry and test setup, see Figure 6.11. Figure 6.12 shows the average results on the form of load-specimen elongation, and Figure 6.13 shows an example of the results from the DIC monitoring, compared with a photo of the cracks from one of the tested specimens.

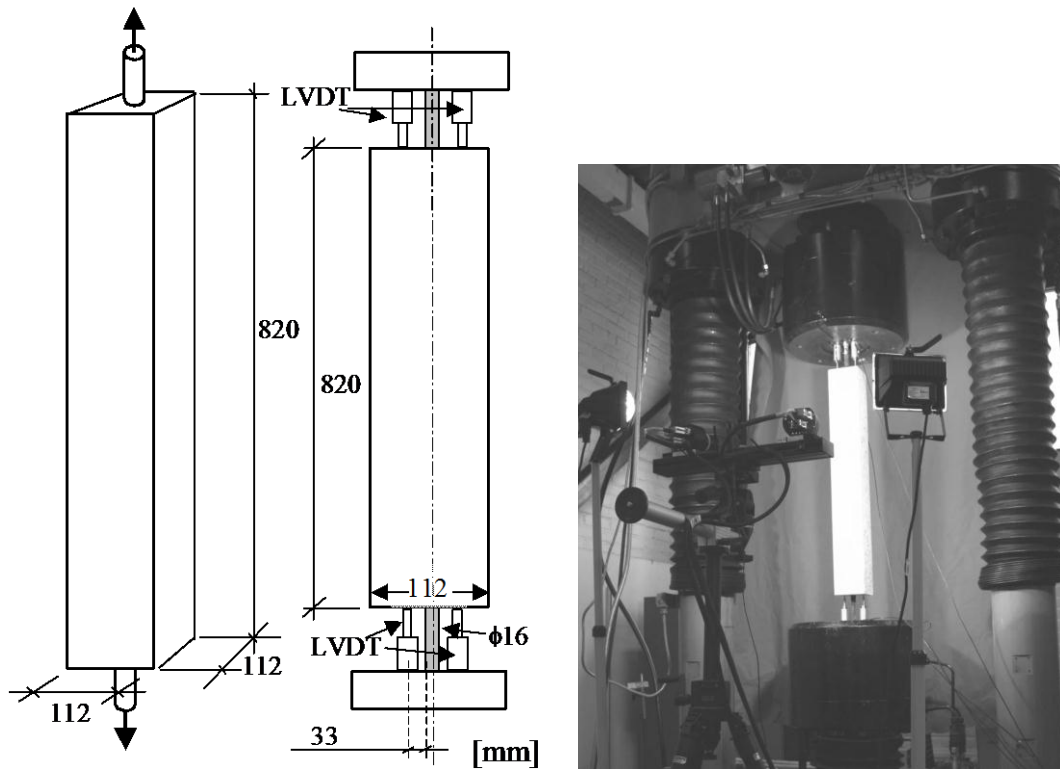


Figure 6.11 Geometry and test setup for the tie element testing.

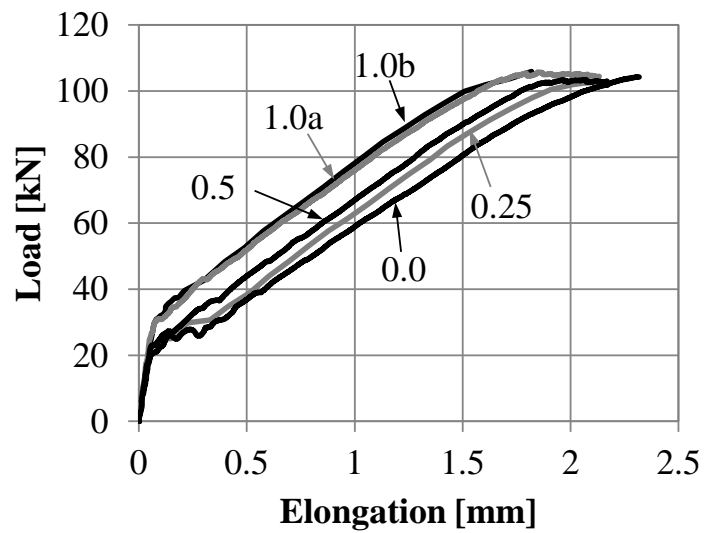


Figure 6.12 Average load-elongation curves for the tested tie elements.

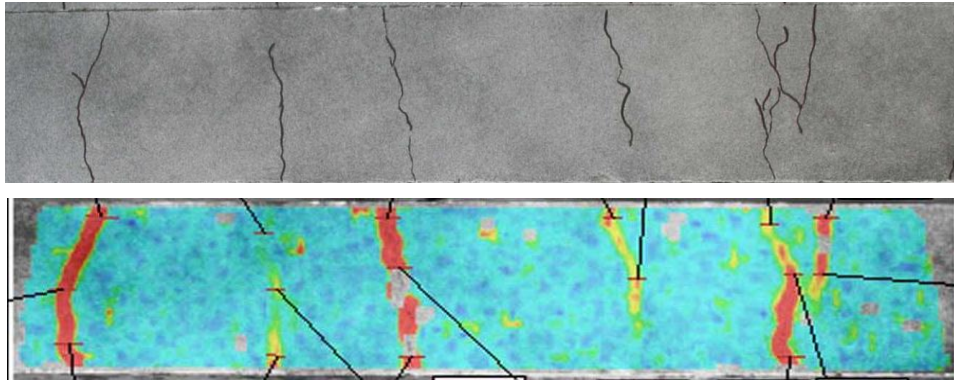


Figure 6.13 Photograph of the final crack pattern in Series 0.5, specimen 4, compared with the crack pattern obtained with the DIC system.

6.7 Tie Element Testing: Non-Linear Analysis

The tie elements were analyzed using 3D models, in which the results from the previously described pull-out and UTT, were used as input. Two mesh sizes were used, a fine and a rather coarse one, see Figure 6.14. The FEA of the tie elements is reported in Paper V.

For Series 0.0 the given choice for the crack band width, h , would be the same as the element size: $h = 10$ or 29 mm, depending on the mesh used. For the coarse mesh, $h = 29$ mm, yielded acceptable agreement with experimental load-elongation and number of cracks; $h = 58$ mm showed good agreement. For the fine mesh, the choice of $h = 10$ mm (i.e. one element width) yielded 4 cracks, but overestimated the load-elongation curve. When the crack band width was increased to $h = 20$ mm, and $h = 40$ mm, better agreement was achieved for the load-elongation curve. Figure 6.15 shows the load-elongation curves for different choices of crack band width.

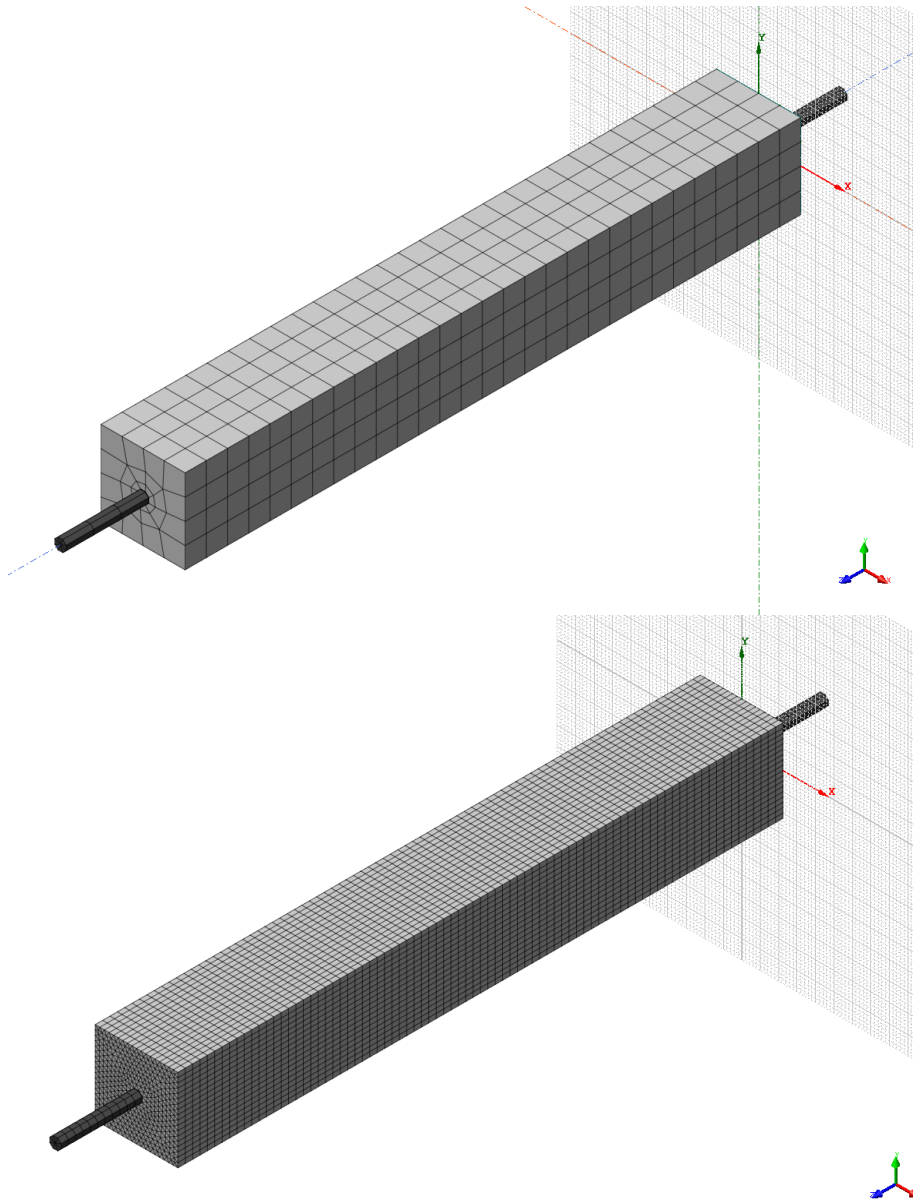


Figure 6.14 The two models used: top – coarse mesh with element height of 29mm, and bottom – fine mesh with element height of 10mm.

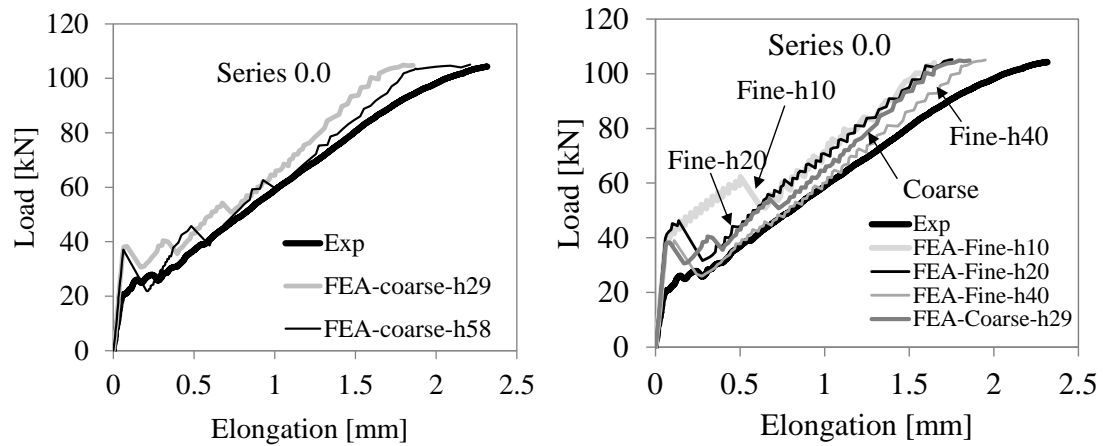


Figure 6.15 Series 0.0, effect of different crack band width on the load-elongation curve.

Furthermore, it was seen in the analyses; if the fibre content was high, the assumption of homogenous distribution of material strengths was incompatible with the smeared cracking model. That is, for an initial residual tensile stress which is only slightly lower than the maximum tensile stress, the reduction in stress-transferring capacity in a cracked element is too small for the adjacent elements to become unloaded. This effect was observed in Series 1.0a and 1.0b. To overcome the localization problem, the material behavior was modified such that, a distribution between two cases of materials, was obtained. The modification was based on observations of the fibre distribution, and the size of the finite element, according to the following procedure:

After testing, the tie elements were cut at three locations, and the number of fibres in the cross sections was counted. For Series 1.0b, the average number of fibres / $\text{cm}^2 \approx 1.7$ and for Series 1.0a the average number of fibres / $\text{cm}^2 \approx 2$. For simplicity it was assumed that the average for both series was equal to 2 / cm^2 . The area of one triangular mesh element was:

$$A_{elem} = \frac{6.2 \cdot 5.4}{2} = 16.74 \text{ mm}^2 \quad (6.2)$$

There is room for 6 element areas within one square centimeter, thus, two of these elements may contain one fibre each, and the remaining four elements will be “empty”. This means that two thirds of the elements are plain. The idea was to model this by assigning $2/3$ of all elements properties for plain concrete. By this action the average capacity would be reduced, and due to this, the remaining $1/3$ would have to be assigned modified properties to compensate for the, otherwise, reduced average capacity. The modification was applied on the σ - w relationship based on the following:

$$\sigma_{exp} = \frac{2}{3} \sigma_{plain} + \frac{1}{3} \sigma_{modified} \quad (6.3)$$

$$\sigma_{modified} = 3\sigma_{exp} - 2\sigma_{plain} \quad (6.4)$$

The calculations were carried out on the experimental data: the average stress-displacement (σ - δ) curves from the UTT. Figure 6.16 shows the modified stress-

displacement curves for Series 1.0b. The crack width is obtained by deducting the elastic part from the total displacement, see Paper III. Figure 6.17 shows the modified stress-crack width relationship for Series 1.0a. Figures 6.18-6-20 show the elements with different material properties.

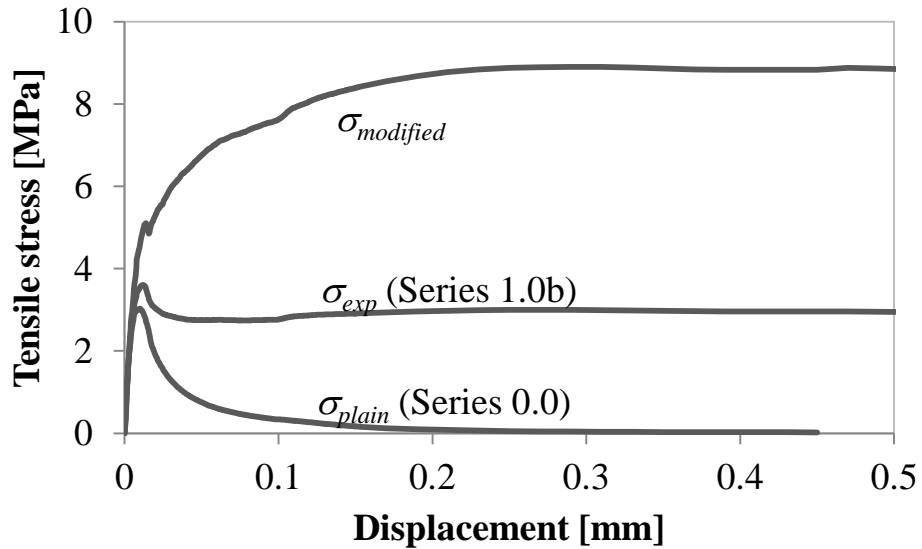


Figure 6.16 Modified stress-displacement for Series 1.0b obtained from Equation (6.4).

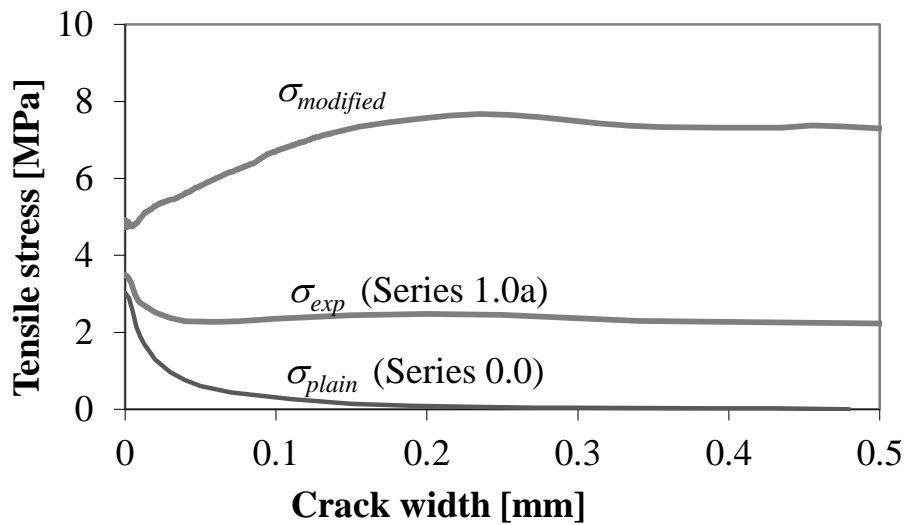


Figure 6.17 Modified stress-crack width for Series 1.0a obtained from Equation (6.4).

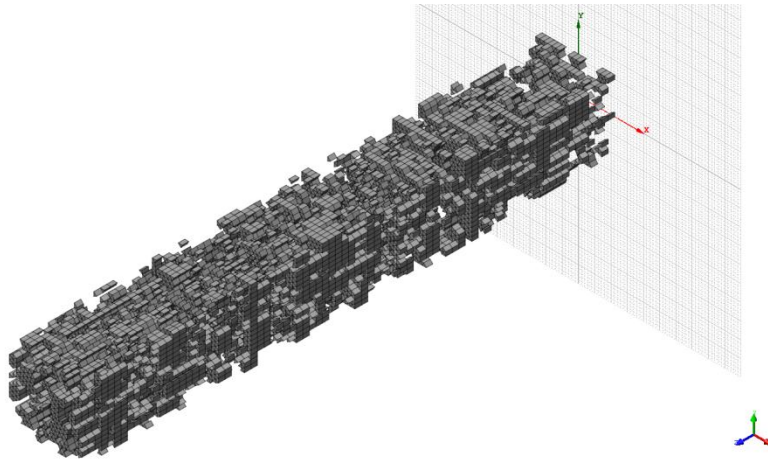


Figure 6.18 Mesh with modified elements.

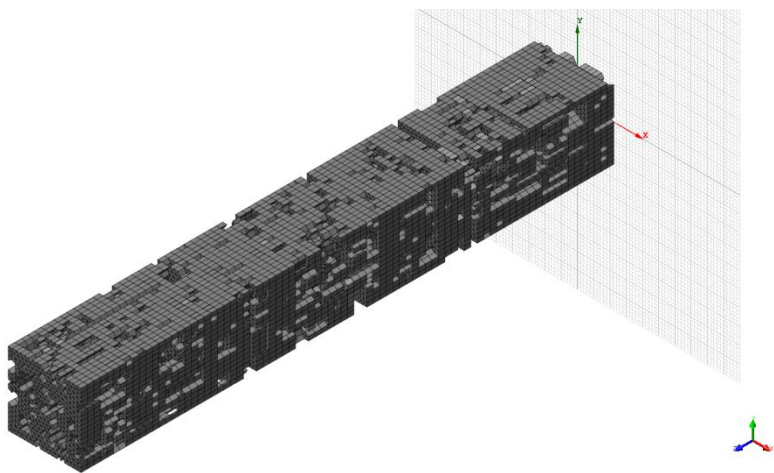


Figure 6.19 The mesh elements with properties for plain concrete.

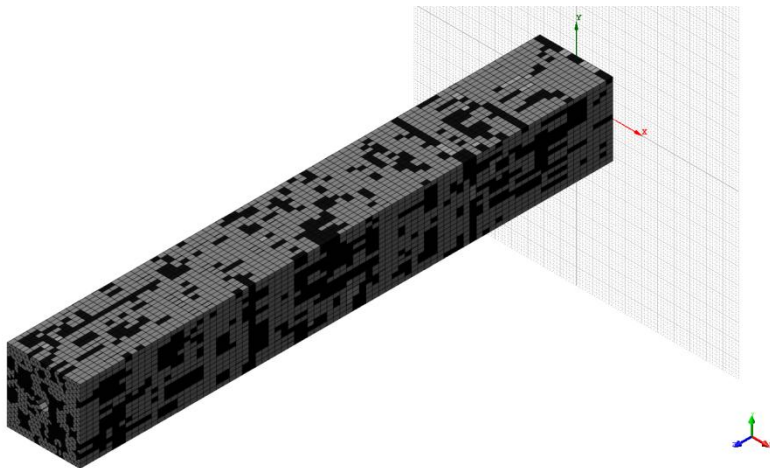


Figure 6.20 The complete concrete mesh. Dark elements have modified properties.

7 Discussion

The stress-crack opening curve represents the energy that is consumed/dissipated during the fracture process and the crack-band width is used to convert the crack width (or displacement) to a strain. When modelling concrete without fibre reinforcement and assuming complete interaction between concrete and rebars, the crack-band width is chosen as the average crack spacing. If instead allowing slip between concrete and rebars, the crack-band width is usually chosen as the width (or average width) of one mesh element, assuming that the crack should localize within this element row only. For fibre reinforced concrete, on the other hand, this choice is not as straight forward. Conventional reinforcement in combination with fibre reinforcement may create a densely distributed reinforcement, which gives rise to diffusion and distortion in the neighbourhood of the reinforcement, and lead to a diffuse crack pattern. The reason for this is that the fibres are able to transfer significant stresses across the crack. This means that even if the elements neighbouring the actual crack might not be subjected to localised cracking, they are subjected to large stresses due to the stress transfer across the crack, and micro cracks may be present. Due to this the crack pattern in analyses of fibre-reinforced concrete becomes more diffuse than for concrete with no fibres added, and the assumption of crack localization in one element row might not hold. It then seems reasonable that the crack band width for FRC materials with combined reinforcement instead could be chosen closer to the average crack spacing. In order to ensure the toughness to be correctly modelled, the energy needed to crack one unit area, is thus averaged out over several element widths (i.e. a larger crack-band width is used). This is also necessary in order to make sure that the load bearing capacity, i.e. the stress transfer over the crack is not overestimated. If the crack band width is chosen too small, the load bearing capacity may be overestimated. This is a difficulty when modelling FRC materials and further investigations regarding this matter are necessary. When modelling the beam-bending tests, the size of one quadratic mesh-element in the 2D model was $5 \times 5 \text{ mm}^2$. In Figure 7.1 different values of the crack band width h , were adopted for the analyses of the beam-bending tests in experimental programme one; it is seen that the peak load increases with decreasing h .

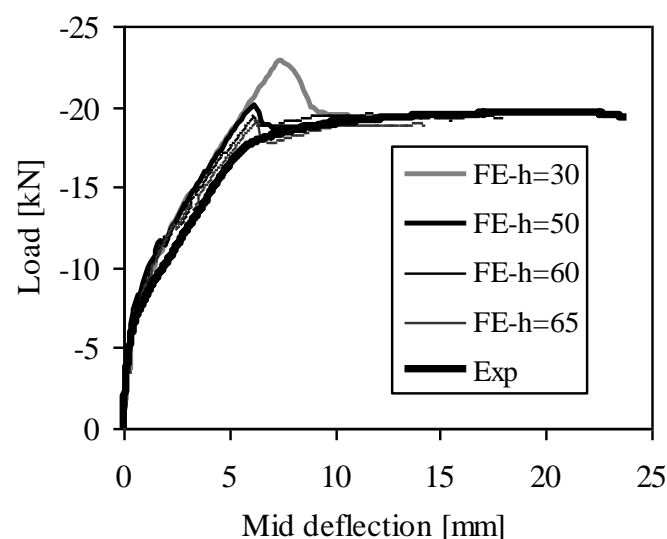


Figure 7.1 Results from 4-point beam-bending test for Series 0.5- ϕ ; h in mm.

When analyzing the pull-out tests, it was investigated how different choices of h , would affect the results. Figure 7.2-7.3 show the bond stress-slip results for Series 0.0 and 0.5, when using $h = 6.2\text{mm}$ and $h = 12.4\text{mm}$. Figure 7.4 shows the effect on the σ - ε curve from the two choices of h for Series 0.5. For all pull-out analyses the width of one mesh-element was 6.2mm .

It is seen in the figures that, although there is a small, but noticeable, difference at peak load and close thereafter, both choices seem reasonable. Since the main focus was cracking in the early loading stage, and also since the fibre content in Series 0.0, 0.25 and 0.5 was relatively small, it was assumed appropriate to adopt the usual assumptions used for plain concrete regarding the choice of crack-band width (i.e. $h = 1$ mesh-element width). For the remaining two series (1.0a and 1.0b), the same choice was made ($h = 6.2\text{mm}$).

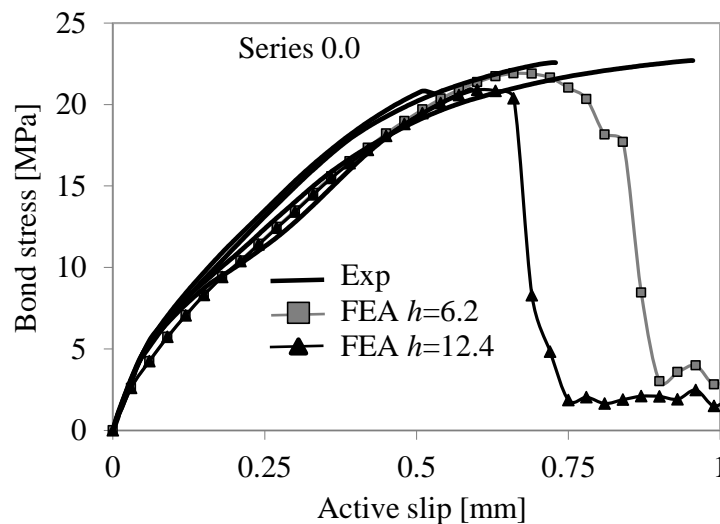


Figure 7.2 Effect of crack-band width h , on the bond stress-slip curves from the pull-out tests. The fibre-volume fraction $V_f = 0\%$.

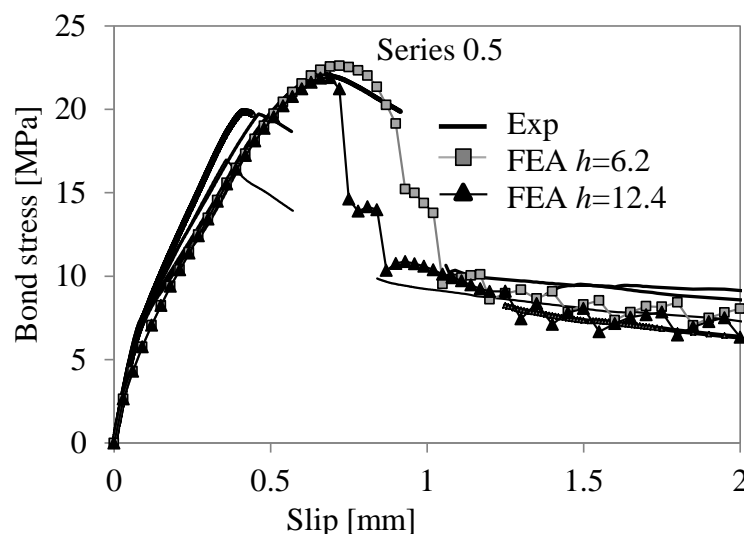


Figure 7.3 Effect of crack-band width h , on the bond stress-slip curves from the pull-out tests. The fibre-volume fraction $V_f = 0.5\%$.

As an example, starting from the measured σ - w relationship for Series 0.5; to obtain the same strain value for $h = 12.4$ as for $h = 6.2$ mm, a larger value of the crack (w) is needed; thus, if adopting $h = 12.4$ mm the stress reduction after peak is reached faster. The effect is largest in the very beginning, but this is also where it may have the most impact on the results; at strain = 0.005 the stress reduction, from $h = 6.2$ to $h = 12.4$ mm, is 20%. Figure 7.5 shows the effect from three different values of h when deriving the σ - ε relationship for Series 1.0b; it is seen that the initially high residual stress is not meaningfully affected for small values of h . Here the stress reduction at strain = 0.005 is only 0.6% between $h = 6.2$ and $h = 12.4$ mm. Even if using the unrealistic value $h = 120$ mm, it is seen that the stress doesn't start to decrease in a meaningful way until $w > 0.76$ mm (Figure 7.5); and looking at Figure 7.6, it is seen that there is barely no difference between using $h = 6.2$ and $h = 12.4$ mm. When $h = 120$ mm there is a meaningful difference, however, as already pointed out, this value is unrealistic.

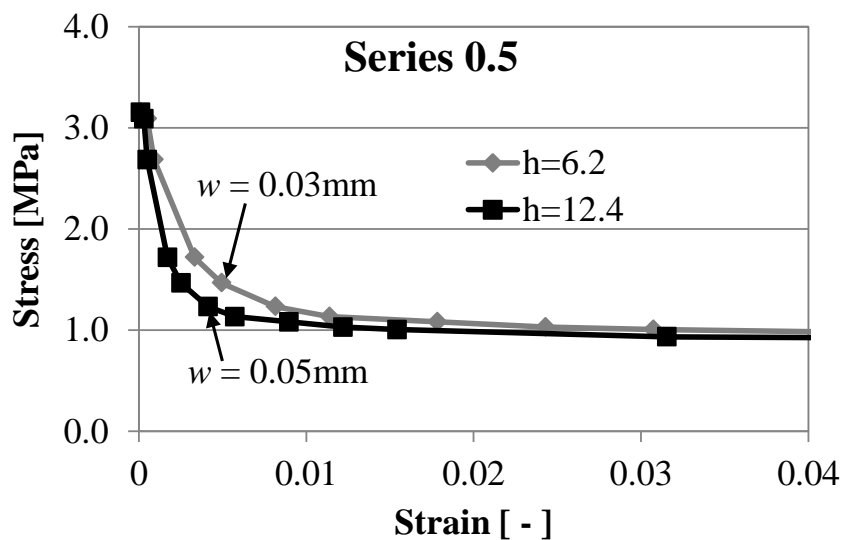


Figure 7.4 Translating the σ - w curves from the pull-out tests to σ - ε curves. Effect of the crack-band width h , with nominal fibre-volume fraction $V_f = 0.5\%$.

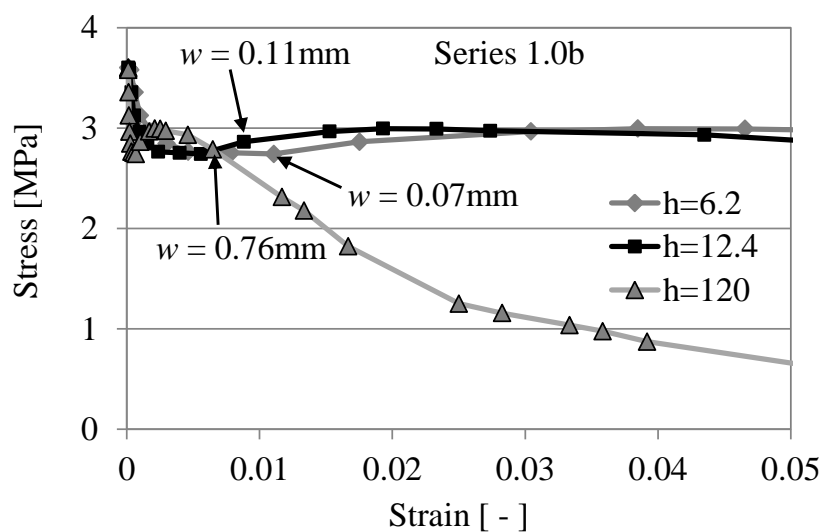


Figure 7.5 Translating the σ - w curves from the pull-out tests to σ - ε curves. Effect of the crack-band width h , with nominal fibre-volume fraction $V_f = 1.0\%$.

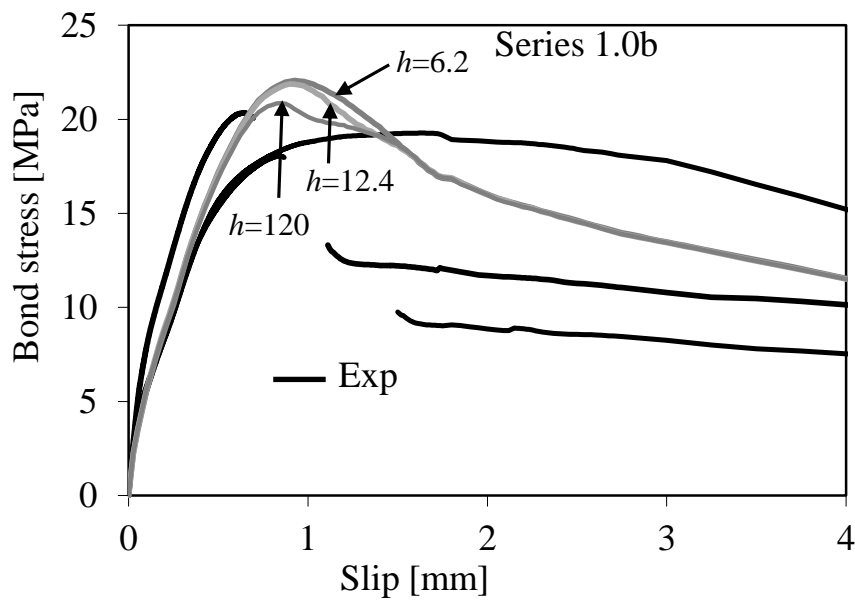


Figure 7.6 Effect of crack-band width h , on the bond stress-slip curves from the pull-out tests. The nominal fibre-volume fraction $V_f = 1.0\%$.

8 Conclusions and Future research

8.1 General Conclusions

The aim with the work was to deepen the knowledge of the cracking process in fibre reinforced concrete; and, if possible, also find a method to predict the crack widths in the serviceability limit state. The methodology used was experiments in combination with non-linear finite element analysis, which proved useful. Regarding the experiments, it should be mentioned that the test equipment, which was developed together with the Technical Research Institute of Sweden, SP, for the uniaxial tension tests, proved successful, and the tests were carried out successfully. Also the pull-out tests with short embedment length, and the tie element tests, were conducted satisfactorily.

From the experiments the following conclusion may be drawn:

- For the self-compacting concrete used in this investigation it was found that increasing fibre content in the UTT specimens resulted in, not only increased residual tensile strength, but also the first peak stress increased;
- The pull-out tests (with short embedment length) showed that the inclusion of fibres, for the herein used fibre type and amounts, had no effect on the initial bond stiffness or on the bond strength;
- After cracking, the fibres provided a confining effect, which could be compared with the one from transversal reinforcement;
- The tension stiffening effect was markedly improved by fibre reinforcement, which is not recognized in MC 2010, and the tension stiffening effect (represented by the bond factor β) is almost constant with increased member strain/load compared to the observed degradation which occurs for plain concrete;
- The crack spacing was reduced and the characteristic crack widths turned out to be significantly reduced by the fibres;
- The DIC technique used, proved useful for monitoring the cracks during the cracking process; and it was found that the inclusion of fibres reduced the initial sudden crack opening (caused by elastic unloading);
- Through the DIC technique, the tension stiffening could be quantified, by relating it to the characteristic crack width.

When using the type of crack model that was applied in the finite element analyses, there is a difficulty; a length over which the crack should be smeared out must be estimated. The fibres induce a zone over which stress transfer still occurs, as opposed to conventional plain concrete, and this might cause a need for larger choice of crack band width. This was investigated and discussed, but no clear conclusions regarding the crack band width could be drawn. Following was found through the analyses:

- The bond model used in the analyses proved versatile, and, in addition to the stresses captured in the load direction, for the analyses utilizing a model with fine mesh it also proved capable of capturing the splitting stresses;
- The herein used fibre type, and fibre amounts, did not affect the bond properties at the interface layer, no effect on the peak bond stress and the ascending part was observed;
- After cracking, the fibres provided a confining effect (for splitting cracks), which could be compared with the one from transversal reinforcement;

- From the self-compacting concrete, there were indications of an increased initial bond stiffness;
- The general cracking behaviour was well reproduced; while the average crack widths were underestimated;
- It was found that with the suggested semi-meso approach, the agreement between the experiments and the analyses regarding the load-elongation response, improved markedly. Furthermore, with this method crack localization was achieved, however, the number of cracks was underestimated;

The modified semi-meso approach seems promising; however, further investigations are needed.

8.2 Suggestions for Future Research

At present time controlling the fibre distribution seems to be a difficulty when adding fibres to a concrete matrix. If this could be solved in a less costly way than by SIFCON or SEMCON techniques, the reliability of the material properties would increase, and FRC materials would most likely attain more interest from the building industry.

Furthermore, the difficulty with choosing the correct crack-band width when analysing FRC with finite-element analysis, needs to be solved. Possibly non-local models can be utilized so that the choice is no longer necessary; or discrete crack models can be used to obtain the correct choice by back-calculation (inverse analysis). Of interest would also be to use models on a meso-scale, so that the fibre concrete is not modelled as a homogenous material; instead the fibres, the aggregates and the cement paste could be modelled separately within the matrix, with interfaces in between all surfaces.

9 References

- Abid, A. and K. Franzen (2011). *Design of Fibre Reinforced Concrete Beams and Slabs (Preliminary title)*. Master of Science Thesis in the Master's Programme Structural Engineering and Building Performance Design, Department of Civil and Environmental Engineering, Chalmers University of Technology, Gothenburg, will be published in 2011.
- Akkaya, Y., A. Peled and Shah.S.P (2000). Parameters Related to Fiber Length and Processing in Cementitious Composites. *Materials and Structures* 33: pp. 515-524.
- Akkaya, Y., S. P. Shah and B. Ankenman (2001). Effect of Fiber Dispersion on Multiple Cracking of Cement Composites. *Journal of Engineering Mechanics* 127(4): pp. 311-316.
- Ascione, L., V. Berardi, M. di Prisco, C. Failla, A. Grimaldi, A. Meda, Z. Rinaldi, G. Plizzari and M. Savoia (2006). CNR-DT 204/2006, Istruzioni per la Progettazione, l'Esecuzione ed il Controllo di strutture di Calcestruzzo Fibrorinforzato. 59 pp.
- Banthia, N., M. Azzabi and M. OPigeon (1993). Restrained Shrinkage Cracking in Fibre-Reinforced Cementitious Composites. *Materials and Structures* 26: pp. 405-413.
- Banthia, N. and R. Gupta (2004). Hybrid Fiber Reinforced Concrete (HyFRC): Fiber Synergy in High Strength Matrices. *Materials and Structures* 37(10): pp. 707-716.
- Banthia, N. and J. Sheng (1996). Fracture Toughness of Micro-Fiber Reinforced Cement Composites. *Cement & Concrete Composites* 18(4): pp. 251-269.
- Barr, B. I. G. and E. B. D. Hasso (1985). A Study of Toughness Indices. *Magazine of Concrete Research* 37(132): pp. 162-174.
- Barragán, B. E. (2002). *Failure and Toughness of Steel Fiber Reinforced Concrete under Tension and Shear*. Ph.D. Thesis, Universitat Politècnica de Catalunya, Barcelona Spain.
- Barros, J. A. O., V. M. C. F. Cunha, A. F. Ribeiro and J. A. B. Antunes (2005). "Post-Cracking Behaviour of Steel Fibre Reinforced Concrete." *Materials and Structures* 38 pp. 47-56.
- Barros, J. A. O. and J. A. Figueiras (2001). Model for the Analysis of Steel Fibre Reinforced Concrete Slabs on Grade. *Computers and Structures* 79(1): pp. 97-106.
- Bentur, A. and S. Mindess (2006). *Fibre Reinforced Cementitious Composites 2nd Edition* Modern Concrete Technology 15, Taylor & Francis, London and New York, 601 pp.
- Bischoff, P. (2003). Tension Stiffening and Cracking of Steel-Fiber-Reinforced Concrete. *Journal of Materials in Civil Engineering* 15(2): pp. 174-182.
- Burger, R. (2006). *Non-Linear FEM Modelling of Steel Fibre Reinforced Concrete for the Analysis of Tunnel Segments in the Thrust Jack Phase*. Faculty of Civil Engineering and Geosciences, Master in Structural Engineering, Concrete Structures. Delft, 2001, Delft University of Technology.
- Carlswärd, J. (2006). *Shrinkage Cracking of Steel Fibre Reinforced Self Compacting Concrete Overlays*. Ph.D. Thesis. Department of Civil and Environmental

Engineering, Luleå University of Technology, Series no. 2006:55. Luleå, Sweden, 261 pp.

da Cunha (2010). *Steel Fibre Reinforced Self-Compacting Concrete - from Micro-Mechanics to Composite Behaviour*. Ph.D. Thesis, University of Minho, Portugal, 2010.

Dupont, D. (2003). *Modelling and Experimental Validation of the Constitutive Law (σ - ε) and Cracking Behaviour of Fibre Reinforced Concrete*. Ph.D. Thesis. Katholieke Universiteit Leuven, 2003, 256p.

Dössland, Å. (2008). *Fibre Reinforcement in Load Carrying Structures - Laboratory and Field Investigations compared with Theory and Finite Element Analysis*

Ph.D. Thesis, Faculty of Engineering Science and Technology, Norwegian University for Science and Technology, Trondheim, 2008:50, 254 p.

EC2 (1991). ENV-1992-1-1, Eurocode 2: Design of Concrete Structures, Part 1-1: General Rules and Rules for Buildings. . pp.

EC2 (2004). *EN-1992-1-1, EUROPEAN STANDARD. Eurocode 2: Design of Concrete Structures - Part 1-1: General Rules and Rules for Buildings*.

Elsaigh, W. (2007). *Modelling the Behaviour of Steel Fibre Reinforced Concrete Pavements*. Ph.D. Thesis. Civil and Biosystems Engineering, University of Pretoria, Pretoria, 2007.

Ezeldin, A. S. and T. W. Shiah (1995). Analytical Immediate and Long-Term Deflections of Fiber Reinforced Concrete Beams. *Journal of Structural Engineering* 121(4): pp. 727-738.

Fischer, G. and V. Li (2006). Effect of Fiber Reinforcement on the Response of Structural Members. *Engineering Fracture Mechanics* 74: pp. 258-272.

FRC workshop (2007). Fibre-reinforced concrete for strong, durable and cost-saving structures and infrastructures. *FRAMCOS-6*: pp. 163.

Gopalaratnam, V. G., P. Shah, G. Batson, M. E. Criswell, V. Ramakrishnan and M. Wecharatana (1991). Fracture Toughness on Fiber Reinforced Concrete. *ACI Materials Journal* 88(4): pp. 339-353.

Groth, P. (2004). *Fibre Reinforced Concrete - Fracture Mechanics Methods Applied on Self-Compacting Concrete and Energetically Modified Binders*. Ph.D. Thesis. Department of Civil and Mining Engineering, Luleå University of Technology, Series no. 2000:4. Luleå, Sweden, 237 pp.

Grünewald, S. (2004). *Performance-Based Design of Self-Compacting Fibre Reinforced Concrete*, Department of Structural and Building Engineering, Delft University of Technology, Delft, 2001.

Gustafsson, M. and H. Karlsson (2006). *Fibre-Reinforced Concrete Structures-Analysis of Crack Spacing and Crack Width (In Swedish: Fiberarmerade betongkonstruktioner-Analys av sprickavstånd och sprickbredd)*. Masters Thesis, Department of Structural Engineering, Chalmers University of Technology, Göteborg, 2001, 102 pp.

Hillerborg, A. (1980). Analysis of Fracture by means of the Fictitious Crack Model, particularly for Fibre Reinforced Concrete. *The international journal of cement composites* 2(4): pp. 177-184.

- Hillerborg, A. (1983). *Concrete Fracture Energy Tests performed by 9 Laboratories according to a Draft RILEM Recommendation : Report to RILEM TC50-FMC. Rapport TVBM, 3015*. Lund,: 9, [3] bl.
- Hillerborg, A., M. Modeer and P. E. Petersson (1976). Analysis of Crack Formation and Crack Growth in Concrete by Means of Fracture Mechanics and Finite Elements. *Cement & Concrete Research* 6: pp. 773-782.
- Jansson, A. (2007). *Analysis and Design Methods for Fibre Reinforced Concrete: a State-of-the-Art Report*. Göteborg, Dep. of Civil & Environmental Engineering, Div. of Structural Engineering/Concrete structures, Chalmers University of Technology: 196.
- Jansson, A. (2008). *Fibres in reinforced concrete structures, analysis, experiments and design. Civil and Environmental Engineering*. Göteborg, Chalmers University of Technology. Licentiate: 70.
- Kanstad, T. and Å. Dössland (2004). *Testing and Modelling of Steel Fibre Reinforced Concrete Beams Designed for Moment Failure*. . Fracture Mechanics of Concrete Structures, Vol 2. Proceedings of FRAMCOS-5,, Vail, Colorado.
- Kooiman, A. G. (2000). *Modelling steel fibre reinforced concrete for structural design* Technical University of Delft: 184.
- Lambrechts, A. N. (2004). *The variation of steel fibre concrete characteristics. Study on toughness results 2002-2003. In Fibre Reinforced Concrete from Theory to Practice*. International Workshop on advances in Fiber Reinforced Concrete, Sept. 24-25, Bergamo, Italy. pp. 135-148.
- Laranjeira de Oliveira, F. L. (2010). *Design-oriented constitutive model for steel fiber reinforced concrete*. Ph.D. Thesis, Universitat Politècnica de Catalunya, Barcelona, Spain, 2010, 218p.
- Li, V. C., D. K. Mishra and H. C. Wu (1995). Matrix Design for Pseudo Strain-Hardening Fiber Reinforced Cementitious Composites. *Materials and Structures* 28(183): pp. 586-595.
- Lok, T. and J. Xiao (1999). Flexural Strength Assessment of Steel Fiber Reinforced Concrete. *Journal of Materials in Civil Engineering*, 11(3): pp. 188-196.
- Lok, T. S. and J. S. Pei (1998). Flexural Behaviour of Steel Fiber Reinforced Concrete. *Journal of Materials in Civil Engineering* 10(2): pp. 86-97.
- Lundgren, K. (2005). Bond between Ribbed Bars and Concrete. Part 1: Modified Model. *Magazine of Concrete Research* 57(7): pp. 371-382.
- Lundgren, K. and K. Gylltoft (2000). A Model for the Bond between Concrete and Reinforcement. *Magazine of Concrete Research* 52(1): pp. 53-63.
- Löfgren, I. (2005). *Fibre-reinforced Concrete for Industrial Construction-a fracture mechanics approach to material testing and structural analysis*. Ph.D. Thesis. Department of Structural Engineering, Chalmers University of Technology, New Series no. 2378. Göteborg, Sweden, 2001, 243 pp
- Löfgren, I. (2007). *Calculation of Crack Width and Crack Spacing. Nordic Mini Seminar "Fibre reinforced concrete"*. Trondheim, Norway.

Löfgren, I., J. F. Olesen and H. Stang (2004). *Wedge Splitting Test – A Test to Determine Fracture Properties of FRC*. 6th RILEM symposium fibre reinforced concretes (FRC) – BEFIB 2004. Varenna, Italy, pp. 379-388.

Magnusson, J. (2000). *Bond and Anchorage of Ribbed Bars in High-Strength Concrete*. Ph.D. Thesis. Department of Structural Engineering, Chalmers University of Technology, Publication no. 00:1, Göteborg, Sweden, 299 pp.

Model Code 90 (1999). *Textbook on behaviour, Design and Performance, CEB/FIP, Updated knowledge-bulletin 1*, International Federation for Structural Concrete (fib).

Model Code (2010). *CEB-FIP, Bulletin 56, FIB 2010, First Complete Draft, Vol 2*. Published by International Federation for Structural Concrete (fib).

Naaman, A. E. and H. W. Reinhardt (1996). *High Performance Fiber Reinforced Cement Composites. HPFRCC 2, RILEM*. Vol. 31, 505 pp.

Naaman, A. E. and H. W. Reinhardt (2006). Proposed Classification of HPFRC Composites based on their Tensile Response. *Materials and Structures* 39: pp. 547-555.

Pereira, E. N. B., J. A. O. Barros, A. Ribeiro, F. and A. Camões (2004). *Post-Cracking Behaviour of Self-compacting Steel Fibre Reinforced Concrete*. 6th International RILEM Symposium on Fibre Reinforced Concretes, RILEM Publications SARL. pp. 1371-1380.

Plizzari, G. A. and G. Tiberti (2007). *Structural Behaviour of SRFC Tunnel Segments*. Conference proceedings, FRAMCOS-6, Catania, Italy.

Popovic, S. (1973). A Numerical Approach to the Complete Stress-Strain Curve of Concrete. *Cement and Concrete Research* Vol. 3, pp. 583-599.

RILEM (2001). TC 162-TDF, Test and Design Methods for Steel Fibre Reinforced Concrete-Uni-Axial Tension Test for Steel Fibre Reinforced Concrete. *Materials and Structures*. Vol. 34, pp. 3-6.

RILEM (2003). TC 162-TDF, Test and Design Methods for Steel Fibre Reinforced Concrete, σ - ϵ Design Method.(Chairlady L. Vandewalle). *Materials and Structures / Matériaux et Constructions*. Vol. 36, pp. 560-567.

RILEM TC 162-TDF (2002). Design of Steel Fibre Reinforced Concrete using the σ - w Method – Principles and Applications (Chairlady L. Vandewalle). *Materials and Structures*. Vol. 35, pp. 262-278.

Robins, P., S. Austin, J. Chandler and P. Jones (2001). Flexural Strain and Crack Width Measurement of Steel-Fibre-Reinforced Concrete by Optical Grid and Electrical Gauge Methods. *Cement & Concrete Research* 31: pp. 719-729.

Robins, P. J., S. A. Austin and P. A. Jones (2003). Spatial Distribution of Steel Fibres in Sprayed and Cast Concrete. *Magazine of Concrete Research* 55(3): pp. 225-235.

Rossi, P., P. Acker and P. Malier (1987). Effect of Steel Fibres at two Different Stages: the Material and the Structure. *Materials and Structures* Vol. 20, pp. 436-439.

Schumacher, P. (2006). *Rotation Capacity of Self-Compacting Steel Fiber Reinforced Concrete*. Delft, the Netherlands, Delft Technical University, 238 pp.

SIS - Bygg, o. a. (2009). *SS-EN 12390-3:2009*.

- Song, P., S. and S. Hwang (2004). Mechanical Properties of High-Strength Steel Fiber-Reinforced Concrete. *Construction and Building Materials*. Vol. 18, pp. 669-673.
- Sorelli, L., A. Meda and G. Plizzari (2005). Bending and Uniaxial Tensile Tests on Concrete Reinforced with Hybrid Steel Fibers *Journal of Materials in Civil Engineering*. Vol. 17. No. 5, pp. 519-527.
- Sorelli, L. and F. Toutlemonde (2005). *On the Design of Steel Fiber Reinforced Concrete Tunnel Lining Segments. 11th International Conference on Fracture*. Turin, Italy, 6 pp.
- Susetyo, J. (2009). *Fibre Reinforcement for Shrinkage Crack Control in Prestressed, Precast Segmental Bridges*. Ph.D. Thesis. Department of Civil Engineering, University of Toronto, Toronto, Canada, 2001. 532 pp.
- Swedish Concrete Society (1997). (In Swedish: Svenska Betongföreningen). *Steel-fibre concrete-recommendations for construction, performance and testing*. Report no4 (In Swedish: Stålfiberbetong-rekommendationer för konstruktion, utförande och provning. Rapport nr 4 - utgåva 2), 135 pp.
- Thorenfeldt, E., T. Sandaker, D. Bosnjak, T. Martinsen, O. Olsen, M. Maage and S. Fjeld (2006). *Veiledning stålfiberarmert betong, Draft 2006*, 42 pp.
- Tlemat, H., K. Pilakoutas and K. Neocleus (2006). Modelling of SFRC using Inverse Finite Element Analysis. *Materials and Structures* Vol. 39, No. 2, pp. 197-207.
- TNO (2005). DIANA - Finite Element Analysis, User's Manual release 9.
- TNO (2011). *Diana, Finite element analysis, User's Manual, release 9.4.3*. Delft.
- Vandewalle, L. (2000). Cracking Behaviour of Concrete Beams Reinforced with a Combination of Ordinary Reinforcement and Steel Fibers. *Materials and Structures* Vol. 33, pp. 164-170.
- Vandewalle, L. (1992). *Theoretical Prediction of the Ultimate Bond Strength between a Reinforcement Bar and Concrete. International Conference: Bond in Concrete from Research to Practice*. Riga, Latvia. Proceedings Vol. 1, pp. 1-1 to 1-8.
- Voo, J. Y. L. and S. J. Foster (2003). *Variable Engagement Model for Fibre Reinforced Concrete in Tension*, School of Civil and Environmental Engineering, University of New South Wales, Australia, 87 pp.
- Workshop proceeding no 2 (2001). Design of Steel Fibre Reinforced Concrete Structures Stockholm, Sweden, June 12, 2001.
- Workshop proceeding no 4 (2003). *Design Rules for Steel Fibre Reinforced Concrete Structures*, Oslo, Norway, October 2003, 14 papers, One Volume, pp.141.
- Zhang, J. and H. Stang (1998): Applications of Stress Crack Width Relationship in Predicting the Flexural Behaviour of Fibre-Reinforced Concrete. *Cement and Concrete Research*, Vol. 28, No. 3, pp. 439-452.